Journal of Drug Delivery Science and Technology 76 (2022) 103735

Contents lists available at ScienceDirect

Journal of Drug Delivery Science and Technology

journal homepage: www.elsevier.com/locate/jddst

Development of triphala churna extract mediated iron oxide nanoparticles as novel treatment strategy for triple negative breast cancer

Ankita Parmanik [a], Anindya Bose [a,*], Bhavna Ghosh [a,b], Milan Paul [c], Asif Itoo [c], Swati Biswas [c], Manoranjan Arakha [d]

[a] School of Pharmaceutical Sciences, Siksha O Anusandhan (Deemed to be University), Bhubaneswar, Odisha, 751003, India
[b] Sri Jayadev College of Pharmaceutical Sciences, Naharkanta, Via: Balianta, Bhubaneswar, Odisha, 752101, India
[c] Department of Pharmacy, Birla Institute of Technology & Science-Pilani, Hyderabad Campus. Jawahar Nagar, Kapra Mandal, Medchal District, Telangana, 500 078, India
[d] Center for Biotechnology, Siksha O Anusandhan (Deemed to be University), Bhubaneswar, Odisha, 751003, India

ARTICLE INFO

Keywords:
Triphala churna
Green synthesis
Iron oxide nanoparticles
Triple negative breast cancer cells
Apoptosis
Anticancer activity

ABSTRACT

The present work demonstrates the eco-friendly green synthesis of Iron oxide nanoparticles from the aqueous extract of Triphala churna (TIONPs) using ferric chloride hexahydrate ($FeCl_3.6H_2O$) precursor in a single-step process. The formulated TIONPs were characterized by various instrumental techniques such as UV–Visible spectrophotometry (UV–Vis), Atomic absorption spectroscopy (AAS), Fourier transform infrared spectroscopy (FT-IR), X-ray diffraction (XRD), Scanning electron microscope (SEM), Dynamic light scattering- Zeta potential (DLS-Zeta sizer), and Superconducting quantum interference device (SQUID) to establish their physico-chemical characteristics. The average size range of obtained spherical TIONPs was found in between 29 and 74 nm. Further, the MTT assay and Nuclear staining assay were carried out on Triple negative breast cancer (TNBC) cell lines along with a breast cancer associated epidermoid skin carcinoma cell line. The MTT assay revealed prominent cytotoxic activity of TIONPs against the tested cancer cell lines. Additionally, the nuclear staining assay revealed that the cytotoxic activity of these nanoparticles occurred via apoptosis mode by exhibiting nuclear fragmentation, cytoplasmic shrinkage, and cell blebbing. These TIONPs were also found to possess superparamagnetic property which may be additionally beneficial for their rapid and organ targeted delivery. Hence, the green synthesized TIONPs can be explored in near future as a new promising option for TNBC management.

1. Introduction

Cancer is considered as a significant cause of death worldwide. The initiation of cancer is very fast and can rapidly spread to the other healthy cells and tissues of the body. Among various cancers, breast cancer is considered as the second most cause of death globally. Breast cancer accounts for about 14% of cancer in Indian women. A report on breast cancer statistics has confirmed that the new breast cancer cases had risen to 1,62,468 in 2018, and the death rate was estimated as 87,090 [1]. Conventional chemotherapeutic drugs experience some limitations in distinguishing between normal and cancerous cells, leading to systemic toxicity and severe side effects [2].

Triple-Negative Breast Cancer (TNBC) is a type of breast cancer that is aggressive and prone to rapid multiplication at the lymph nodes and has a higher chance of recurrence [3]. Once cancer spreads to the lymph nodes or other parts of the body the chances of survival rate of a patient is greatly reduced. It has been reported that the TNBC can grow very faster and eventually spread to a great extent at the time of its diagnosis [4]. As the three prominent women's hormonal receptors (Progesterone, Estrogen and Human epidermal growth factor) are not present in TNBC, hormone therapy or immunotherapy are excluded from the list of treatments for TNBC. Hence chemotherapy using taxanes, anthracyclins, PARP inhibitors, etc. remains the major treatment against TNBC. Unfortunately, inherited cytotoxic activity, non-targeted delivery, and higher doses of these chemotherapeutic drugs result in severe systemic side effects and poor prognosis and the destruction of a large number of healthy cells compared to the TNBC cells. Therefore, it is the high time to implement advanced and novel strategies like nanotechnology in the

* Corresponding author.
E-mail address: anindyabose_in@yahoo.com (A. Bose).

https://doi.org/10.1016/j.jddst.2022.103735
Received 5 June 2022; Received in revised form 12 August 2022; Accepted 20 August 2022
Available online 27 August 2022
1773-2247/

treatment and control of TNBC [5].

In the last few decades, the demand for nanoparticles in the biopharmaceutical application has risen tremendously. Among various nanoparticles, Iron oxide nanoparticles (IONPs) is considered as the most efficient in cancer diagnosis and treatment due to some specific physical and chemical properties. IONPs has so many unique features like superparamagnetism, good tissular diffusion, and better bioavailability with low toxicity. In this regard, IONPs are gaining popularity in various biomedical fields due to their effective size control phenomena, surface characterization along with unique superparamagnetism property [6,7]. In recent years, the IONPs based nano-medicines have been applied for advanced detection, diagnosis, treatment and control of breast cancer related deaths [8,9]. The iron nanoparticles synthesized by chemical methods use many hazardous chemicals which are toxic and unsafe to the environment as well as for the users. However, the latest trend of their green synthesis can replace the use of external chemicals by providing naturally available reducing, capping agents for the reduction of the iron ions [1].

Triphala has been used as a familiar Ayurvedic formulation since ancient times containing an equiproportional mixture of three medicinal fruits: Amlaki (*Emblica officinalis*), Haritaki (*Terminalia chebula*) and Bibhitaki (*Terminalia bellirica*) [10–12]. It is considered as a general well-being medicine that helps to treat numerous illnesses like iron deficiency, cancer, jaundice, obstruction, asthma, fever, persistent ulcers, ongoing blockage, absorption issues, cardiovascular infection, hypertension sickness, decreased serum cholesterol, helpless liver capacity, internal organ irritation, etc. [13–15].

The Triphala churna (powder) affirms the presence of many valuable phytoconstituents such as gallic acid, ellagic acid, chebulinic acid, L-ascorbic acid, alkaloids, bellaricanin, beta-sitosterol, flavonoids (Quercetin, Luteolin etc), saponins, amino acids and so forth which shows strong antioxidant and anticancer activities [16]. Recently, Triphala has also demonstrated potent anticancer activity in HeLa (cervical adenocarcinoma), PANC-1 (pancreatic adenocarcinoma), and MDA-MB-231 (triple-negative breast carcinoma) cells [17]. Prasad et al. observed that the treatment with the aqueous extract of Triphala churna reduces cell proliferation of breast and prostate cancer cells [18]. They suggested that the anticancer activity of Triphala churna is contributed by its polyphenols, ascorbic acid and flavonoids. In another investigation, the anti-proliferative impact of Triphala extract act against MCF-7 breast cancer cell line was reported [19]. In spite of these promising reports about the anticancer activity of Triphala churna in breast cancer, including TNBC, the direct administration of crude Triphala churna to the cancer patients may be proven ineffective due to the poor bioavailability of its active phytoconstituents from the powdered mixture of its herbal ingredients as well as it may be inconvenient to administer in such patients [20].

The vast biological activities of Triphala churna have already encouraged the scientific community to develop Triphala churna-mediated metal nanoparticle formulations. A latest research article has reported the silver nanoparticle made from Triphala churna extract as a promising antioxidant, antimicrobial and anti-diabetic agent [21]. However, there is no reports till now regarding the synthesis of IONPs using Triphala churna and evaluation of its efficacy in treating TNBC. Hence, in this present study, an effort is made to develop IONPs from Triphala churna extract and subsequent evaluation of its invitro anticancer activity in TNBC. In addition, in-vitro antioxidant and in-vitro anti-inflammatory activity of green synthesized Triphala mediated IONPs are also evaluated as these effects may act as the fundamental attributes in the anticancer efficacy of TIONPs.

2. Materials and methods

2.1. Materials

Ferric chloride hexahydrate ($FeCl_3.6H_2O$, purity ~98%) was purchased from HIMEDIA Laboratories. All three individual dried fruit components of Triphala such as Amlaki (*Embellica officinalis),* Haritaki (*Terminalia chebula),* and Bibhitaki (*Terminalia bellirica*) were purchased from the local herbal store and authenticated by a botanist. 4′, 6-Diamidino-2-phenylindole dihydrochloride (DAPI), Paraformaldehyde, Dimethyl sulfoxide (DMSO), Methylthiazolyldiphenyl-tetrazolium bromide (MTT), Trypan blue solution, and Fluoromount-G were obtained from Himedia Labs (India). Acridine orange (AO) was obtained from Sigma-Aldrich Chemicals (Mumbai, India). Deionized water was used throughout the synthesis process.

2.2. Cell lines

Human triple-negative breast cancer cell line MDA-MB-231 and human skin cancer cell line A431 were procured from National Centre for Cell Sciences (NCCS, Pune, India). Murine breast cancer cell lines, 4T1 and Human embryonic kidney cells (HEK-293), were procured from the American Type Culture Collection (ATCC, USA). Dulbecco's Modified Eagle Medium (DMEM), Minimum Essential Medium Eagle (MEM), Penicillin streptomycin, Trypsin-EDTA, and Fetal bovine serum (FBS) were purchased from Himedia Labs (India).

2.3. Preparation of aqueous extract of triphala churna

All three herbal ingredients were subjected for grinding followed by sieving through sieve size 60 and mixing in equal proportion to obtain the Triphala churna. The aqueous extract of the churna was prepared by immersing 1 g of finely ground product into 100 mL distilled water and heating it up to 70 °C for 30 min in a temperature-controlled water bath. The resulting extract was allowed to cool and filtered through Whatman filter paper to remove the debris. Finally, the cleared extract was stored under refrigeration for further use.

2.4. Characterization of the triphala churna extract

2.4.1. Total Phenolic Content (TPC)

The aqueous extracts of the Triphala churna and its three ingredients were evaluated separately for the determination of total phenol content according to the Folin–Ciocalteu method using gallic acid as reference standard [22]. Briefly, 1 mL of the different concentration of the extract or gallic acid was mixed with 1 mL of Folin–Ciocalteu reagent and 1 mL of sodium carbonate (2% w/v). The mixture was incubated for 1h at room temperature and the absorbance was recorded using UV–Vis double beam spectrophotometer against a blank at 765 nm. The total phenolic content in mg GAE/g in the extract was calculated (Mean ± S. D., n = 3) by the help of the Gallic acid standard curve (50–500 μg/mL).

2.4.2. Total Flavonoid Content (TFC)

In a clean test tube, 1 mL of the extract was taken along with 4 mL of distilled water and then 0.3 mL of sodium nitrite (5% w/v) was added to it. After 10 min, 0.3 mL aluminium chloride (10% w/v), and 2 mL of 1 M sodium hydroxide were added. The total volume was made up to 10 mL with distilled water with thorough mixing. The absorbance reading was recorded at 510 nm with the help of a UV–Vis spectrophotometer. Total flavonoid content (mg QE/g) was estimated with the help of the quercetin standard curve (25–100 μg/mL) similar to TPC method [23].

2.4.3. HPTLC fingerprinting

The aqueous extracts of Triphala churna and its all three components were applied on a pre-coated silica gel $60F_{254}$ Aluminium plate (10 cm × 10 cm) with 0.2 mm thickness by the Linomat 5 sample application system (CAMAG) [24]. The plate was then placed in CAMAG glass twin trough developing chamber previously saturated with the mobile phase of Toluene: Ethyl acetate: Formic acid: Methanol (3: 2.6: 0.4: 4). The developed plate was dried and the retention factor (R_f) values of the developed spots were noted under specified wavelengths (254 nm, 366

nm and 540 nm). The High performance thin layer chromatography (HPTLC) finger print data were documented by winCAT software (CAMAG).

2.5. Green synthesis of triphala mediated iron oxide nanoparticles (TIONPs)

Ferric chloride hexahydrate ($FeCl_3.6H_2O$) was used as precursor salt to synthesize TIONPs. The specific amounts of Ferric chloride hexahydrate (1 mM) was directly added to the 100 mL of aqueous churna extract (10 mg/ml) with a constant stirring at 600–700 rpm by a magnetic stirrer at room temperature. The pH of the mixture was adjusted to 11 by adding alkali solution, and the reaction mixture was constantly stirred for 30 min for complete synthesis. Gradually, the colour was changed from reddish-orange to intense black, which confirmed the formation of TIONPs. After completing the synthesis, the solution was centrifuged at 12000 rpm for 20 min and cleansed by repeated washing with distilled water 2–3 times to remove the impurities. The nanoparticles were collected in a pellet form and dried in a hot air oven at 60 °C for 3 h and stored in a tube for further use. Finally, the percentage yield of synthesized TIONPs was calculated as per the standard method [25].

2.6. Effect of time and pH condition on the synthesis of iron oxide nanoparticles

In order to optimize the quality of the developed TIONPs, the effect of main operational parameters of synthesis such as time and pH were studied by adopting variations in the experimental conditions. The pH of the reaction mixture was adjusted with 0.1 N HCl or 1 M NaOH solution to set three different pH conditions (pH 3, pH 8 and pH 11). Similarly, the effect of reaction time was evaluated by variation in synthesis time at pH 11 (optimum pH condition) to prepare four different grades of TIONPs such as A1 (30 min), A2 (60 min), A3 (120 min) and A4 (360 min).

2.7. Analytical characterization of TIONPs

The characterization of optimized TIONPs was done by various analytical techniques to assure their size/particle size distribution, shape, porosity, aggregation, zeta potential, surface chemistry, crystallinity, colloidal stability, etc. The optical property and completion of reduction of the iron ion was ensured with the help of a double beam spectrophotometer UV–Visible spectroscopy (JASCO V-630 Spectrophotometer) by recording the absorbance spectra. The total iron content in the TIONPs sample was estimated by Atomic absorption spectrometer (Systronics India Ltd, AAS-816) fixed at 248 nm using the calibration curve of ferrous chloride (0.25–1 mg/L) [26]. The functional group detection was conducted by FTIR spectrometer (Jasco-4200, USA) using the KBr pellet method, where the scanning range was kept from 4000 to 400 cm. X-ray Diffraction (XRD) analysis was performed in the 2θ range between 20°-80° with Cu–K radiation and $\lambda = 1.5406$ Å for the determination of their surface characteristics along with the average particle size. The surface morphology of the compounds was determined using Scanning Electron Microscopy (SEM, NOVA NANOSEM 450). The particle size and zeta potential of the synthesized nanoparticles were determined using the principle of dynamic light scattering using Zetasizer 3600 (by Malvern Instruments Ltd. UK). Quantum design Evercool SQUID-VSM (MPMS 3) was employed at room temperature with the varying magnetic field from −10 to +10 kOe to determine of the magnetic property of produced iron oxide nanoparticles.

2.8. Evaluation of in-vitro antioxidant and anti-inflammatory activities

The in-vitro antioxidant activity was evaluated using an ascorbic acid standard by 1, 1-diphenyl-2-picrylhydrazyl (DPPH) free radical scavenging method. Briefly, 2 ml of DPPH methanolic solution (0.1 mM) was mixed thoroughly with the 3 mL of different concentrations (1, 5, 7, 10, 30, 50, and 100 μg/ml) of churna extract or TIONPs solution and incubated at the dark condition for 30 min. Thereafter, the absorbance was recorded at 517 nm in UV–Vis spectrophotometer, and the IC_{50} value was calculated from the ascorbic acid standard curve [27].

The in-vitro anti-inflammatory assay was carried out by the previously reported protein denaturation method [28]. Briefly, 0.02 mL of different concentrations 5–100 μg/ml sample (Triphala churna extract or synthesized TIONPs) solution was mixed thoroughly with 0.2 ml aqueous solution of bovine serum albumin (BSA) (1% W/V) and 4.8 ml of phosphate buffer solution (PBS, pH 6.4). Then they were incubated for 20 min at room temperature and followed by heating at 57 °C for 20 min. Thereafter, the samples were allowed to cool and the turbidity was measured using UV–Vis spectrophotometry at 660 nm. Percentage inhibition of protein denaturation was calculated in comparison with Diclofenac sodium as a standard drug.

2.9. Cell viability study

2.9.1. MTT assay

MTT Assay was performed to determine the cell viability of the TIONPs on different cell lines such as TNBC cell lines (MDA MB231, 4T1), Skin cancer cell line (A431), and normal healthy cell line (HEK 293) using 96 well plates. At first, 100 μl of the cell suspension was added into each well with a concentration of 10,000 cells per well. The plates were incubated in 5% CO_2 at 37 °C for 24 h followed by addition of formulated TIONPs at various concentration (15.62, 31.25, 62.5, 125, 250 and 500 μg/ml). Thereafter, the cells were again incubated for 24 h or 48 h. After this treatment period, 50 μl of MTT reagent (5 mg/ml) prepared in sterile PBS was added into each well and mixtures were again incubated for 4 h prior to addition of 150 μl DMSO to dissolve the formed purple formazan crystals. The absorbance was measured after 1 h at 570 nm and 620 nm using Spectramax Multiplate reader (Molecular Devices, USA).

2.9.2. Nuclear staining assay

Different cancer cell lines (MDA MB 231 cell, 4T1 cells, and A431) were seeded in a 12 well tissue culture plate (50000 cells/well). After 24 h, the cells were treated with various concentrations of all four grades of TIONPs and incubated in 5% CO_2 at 37 °C for 24 h. After incubation, the cells were washed using PBS 7.4, fixed using 4% paraformaldehyde (500 μl/well) and stained using DAPI (10 μg/ml, 90 μl/well) and AO (100 μg/ml, 90 μl/well). These plates were observed under fluorescence microscope at blue channel (358 nm) and green channel (480–490 nm) for DAPI and AO respectively.

3. Results and discussions

3.1. Phytochemical analysis/identification of bioactive constituents

The consumption of phenolic rich foods can minimize the risk factors associated with various types of cancers [29]. In a study with some traditional medicinal plants, Cai et al. (2004) established a positive correlation between antioxidant and total phenolic content with anticancer activity. They revealed significant chemo-preventive potency of traditional plants having strong antioxidant by virtue of their high phenolic content [30].

It is hypothecated that the phenolic compounds can strike the antioxidant levels with applicable in preventing cancer growing cells [31].

Apart from their potential in antioxidant and anticancer activity, phenols and flavonoids can also act as reducing and capping agent for the biocompatible synthesis of nanoparticles [32].

Phenolic compounds, including flavonoids were found to be present in Triphala churna and its all three fruit ingredients. The total phenolic content was estimated using the gallic acid calibration curve y =

0.0017x + 0.0259 (R^2 = 0.9986). It was found that the total phenolic content of Amlaki was maximum (198.85 ± 0.02 GAE/g), followed by Triphala churna, Bibhitaki, and Haritaki with values 67.27 ± 0.08 GAE/g, 55.90 ± 0.02 GAE/g, and 39.17 ± 0.05 GAE/g respectively. Similarly, the total flavonoid content was calculated using Quercetin linear curve: y = 0.0024x + 0.0075 R^2 = 0.9997). The total flavonoid content was seen to be maximum in aqueous extract of Bibhitaki (22.11 ± 0.03 mg Q/g) followed by Haritaki (12.09 ± 0.01 mg Q/g), Triphala churna (7.10 ± 0.01 mg Q/g), and Amlaki (5.48 ± 0.03 mg Q/g). The high phenolic and flavonoid content of Triphala churna, therefore, justifies their utilization in the green synthesis of IONPs for anticancer therapy.

HPTLC, an advanced chromatographic technique having high resolution power, is used to identify the visualizing spots for major active phytoconstituents present in natural products. It can be used as an excellent tool for quality control and standardization of any type of herbal formulation to identify each and every individual ingredients present in an herbal formulation [24].

HPTLC chromatographic 3D fingerprinting analysis of aqueous Triphala extract along with individual ingredients was successfully carried out by CAMAG HPTLC system (Fig. 1) for qualitative standardisation of the Triphala churna formulation. The figure elucidates different visualizing spots on HPTLC silica plates via selected mobile phase at 254 nm, 366 nm and 540 nm. The R_f values of different constituents at 254 nm, 366 nm, and 540 nm (white visible light) are given in Table 1 which confirmed the presence of all the constituents in Triphala churna formulation. The major R_f value for Triphala churna was noticed at 0.88, 0.87, 0.60, 0.53, 0.77, 0.79, 0.72, 0.90 which are contributed from *Embellica officinalis* (0.88, 0.53), *Terminalia chebula* (0.87, 0.60, 0.79), *and Terminalia bellirica* (0.90, 0.77, 0.72).

3.2. Green synthesis and visual inspection of TIONPs

IONPs were prepared by green route using aqueous extract of Triphala churna and the reaction progress was observed through visualization mode. Fig. 2 represents the steps involved in the biosynthesis of TIONPs. The colour of the solution was changed from reddish-orange to lightish black instantly after the addition of churna extract to the iron salt solution which confirmed the reduction of Fe^{3+} ions and subsequent formation of TIONPs. During the process optimization, the maximum UV absorbance peak by the synthesized TIONPs was found at pH 11, indicating that the yield of the synthesized TIONPs is maximum in the alkaline medium. The colour was changed to deep black on stirring the reaction mixture for just 30 min, confirming the rapid formation of TIONPs within this brief reaction time. The % yield of the synthesized TIONPs was found to be 51.85%.

3.3. Characterization of TIONPs

The UV–Visible spectral analysis was conducted to evaluate the absorption spectrum of formulated IONPs for initial confirmation of synthesis. The surface plasmon resonance peaks of TIONPs observed in the 260–280 nm regions were similar to the other reported studies with the IONPs with the maximum light absorption of TIONPs was recorded at 271 nm [33–37]. The comparative UV–Vis spectrophotometric scan of ferric chloride solution, Triphala churna extract, and the synthesized TIONPs solution are elucidated in Fig. 3a. The effect of pH and synthesis time on the yield of synthesized TIONPs are shown in Fig. 3b and c respectively. It is evident that the synthesis is favoured in alkaline medium. Moreover, reaction time of 30 min was enough for complete synthesis of iron oxide nanoparticles from the aqueous extract of Triphala churna. As per this observation, the optimum pH and synthesis time was set at 11 and 30 min respectively. The TIONPs thus formed were processed for further characterizations and evaluation of biological activities. Additionally, the AAS was used to determine the iron concentration present in the formulated nanoparticles (TIONPs) by the help of Ferrous chloride calibration curve (y = 0.0351x- 0.0006, R^2 = 0.9977). The total iron content in the sample was found to be 23.70%.

The FTIR analysis was conducted within 400–4000 cm^{-1} to identify the functional groups responsible for stabilizing and capping of TIONPs. In the FT-IR spectrum (Fig. 4), the 514.90 cm^{-1} peak is attributed to the stretching of Fe–O of Fe_2O_3 or Fe_3O_4 while the peak at 1058.73 cm^{-1} is due to C–O stretching. Moreover, the peak at 1195.65 cm^{-1} denotes the presence of Fe–OH group. The small peak around 1430.92 cm^{-1} is due to the OH stretching and deformation by the water molecular vibration

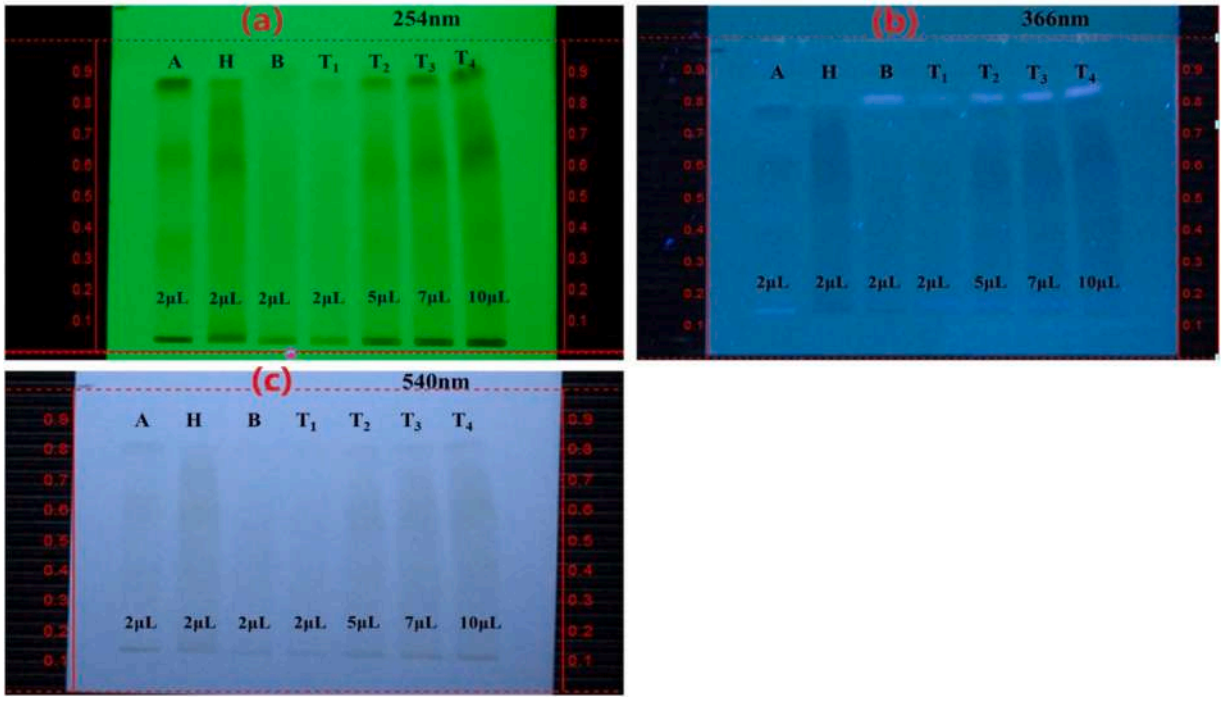

Fig. 1. HPTLC profile of Triphala Churna and its ingredients at (a) 254 nm (b) 366 nm (c) 540 nm [A. *Embellica officinalis* (Amlaki), H. *Terminalia chebula* (Haritaki) B. *Terminalia bellirica* (Bahera), T_1- Triphala churna (2 µL), T_2- Triphala churna (5 µL), T_3- Triphala churna (7 µL), T_4- Triphala churna (10 µL).

Table 1
HPTLC analysis of individual extracts with Triphala churna extract.

R_f Values						
Track 1 (**A- *Embellica officinalis***)	**Track 2** (H- *Terminalia chebula*	**Track 3** (B- *Terminalia bellirica)*	**Track 4** (T_1- Triphala churna 2 μl)	**Track 5** (T_2- Triphala churna 5 μl)	**Track 6** (T_3- Triphala churna 7 μl)	**Track 7** (T_4- Triphala churna 10 μl)
0.88	0.87	0.90	0.86	0.87	0.88	0.90
0.65	0.79	0.84	0.84	0.76	0.79	0.94
0.60	0.60	0.72	0.58	0.60	0.72	0.87
0.53	0.56	0.77	0.81	0.53	0.60	0.77
0.37	0.35			0.36	0.64	0.72
					0.58	0.68

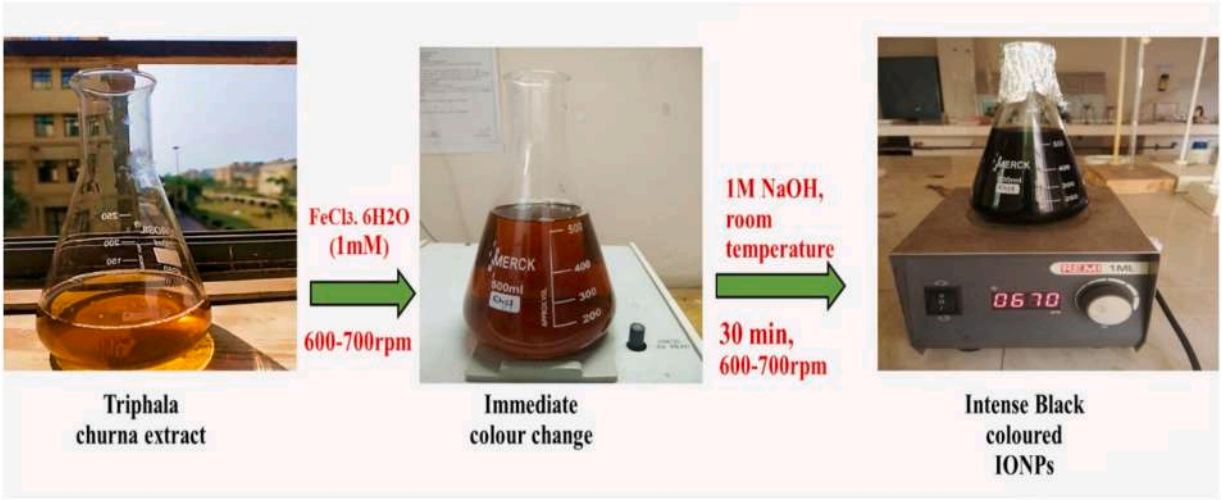

Fig. 2. Steps involved in biosynthesis of TIONPs.

[36,38]. The FT-IR results indicate that prepared IONPs are capped with biologic compounds derived from Triphala churna extract. Additionally, –OH bend of phenol are depicted by an intense peak at 1329.68 cm^{-1} and –C═O peak at 1712.5 cm^{-1} of formulated TIONPs. It also displayed a broad peak of N–H stretch at 3198.36 cm^{-1}. FTIR analysis confirms the presence of amines, phenols, carbonyl, and alkene group that possess a strong binding affinity towards iron and significantly act as reducing and capping agent for the reduction of ferrous ions [39].

X-ray Diffraction (XRD) is an important analytical tool for the examination of the crystalline phase of nanoparticles. The XRD pattern of TIONPs is provided in Fig. 5. The diffraction peaks of hematite nanoparticles (α-Fe_2O_3) are exhibited at 23.38° and 69.72°, while the diffraction peaks at 27.06°, 38.70°, and 55.75°are indicative of the maghemite (γ- Fe_2O_3) nanoparticles [40]. The synthesized IONPs are therefore found to be a mixture of hematite and maghemite nanoparticles [41]. Some other small peaks were observed due to the endorsement of organic materials adsorbed from Triphala extract as capping agents.

The morphological structure of green synthesized TIONPs was examined by scanning electron microscope (SEM). The SEM images (Fig. 6) revealed that the synthesized iron oxide nanoparticles were spherical within the range of 29–74 nm. Zeta potential data represents the stability and electrostatic potential (attraction and repulsion of particles in suspension) of formulated nanoparticles. In our studies, the average particles size distribution and the zeta potential of the synthesized TIONPs measured by DLS- zeta sizer was recorded at −2.95 mV (Fig. 7). Due to the presence of this lower amount of charges on the surface of the TIONPs, there is possibility of agglomeration of nanoparticles. Although, it can be easily tackled by coating these nanoparticles with biocompatible polymer to enhance their stability prior to their utilization in biomedical fields like targeted drug delivery. Moreover, it is also previously reported that the similar low zeta potential can result in formation of stable nanoparticles [42]. The evaluation of hydrodynamic diameter, polydispersity index (PDI), and average particle size of TIONPs was also conducted by DLS (Fig. 7). The narrow size distribution in the range between 35 and 100 nm confirmed the good size reduction of the TIONPs. The intensity peak in the statistics curve revealed that the average particle size of TIONPs was around 167 nm which was suitable enough to cross the biological barriers effortlessly to target a specific site during drug delivery. The PDI value of 0.246 indicated the homogenous distribution of particles within the solution. It is reported that the nanoparticle PDI value lesser than 0.3 is acceptable for their drug delivery applications [43]. Thus, the results clearly demonstrated the monodispersive nature of our synthesized TIONPs.

The magnetic characterization of TIONPs was monitored at room temperature by SQUID-VSM magnetometer (Fig. 8). The results showed the linear M − H graph with no hysteresis loop, which confirmed the paramagnetic nature of synthesized TIONPs [44]. Paramagnetism is a kind of magnetic nature of materials that is weakly attracted by a strong externally applied magnetic field. This paramagnetic property may become helpful to regulate the movement of the TIONPS within body by a strong external magnetic field to facilitate their site specific action [45].

3.4. *In-vitro antioxidant and anti-inflammatory assay*

The active metabolites present in the plant products can exert a wide range of biological activities. The phenolic and flavonoid-like constituents are mainly responsible for the scavenging of free radicals and break the chain of lipid oxidation reaction by phenolic hydroxyl groups [46]. The uncontrolled production of free radicals or reactive oxygen species (ROS) in the body leads for the abnormal epithelial cell growth and ultimately developing the breast cancer [47]. Hence, the antioxidant and anti-inflammatory activity of TIONPs was evaluated in support of

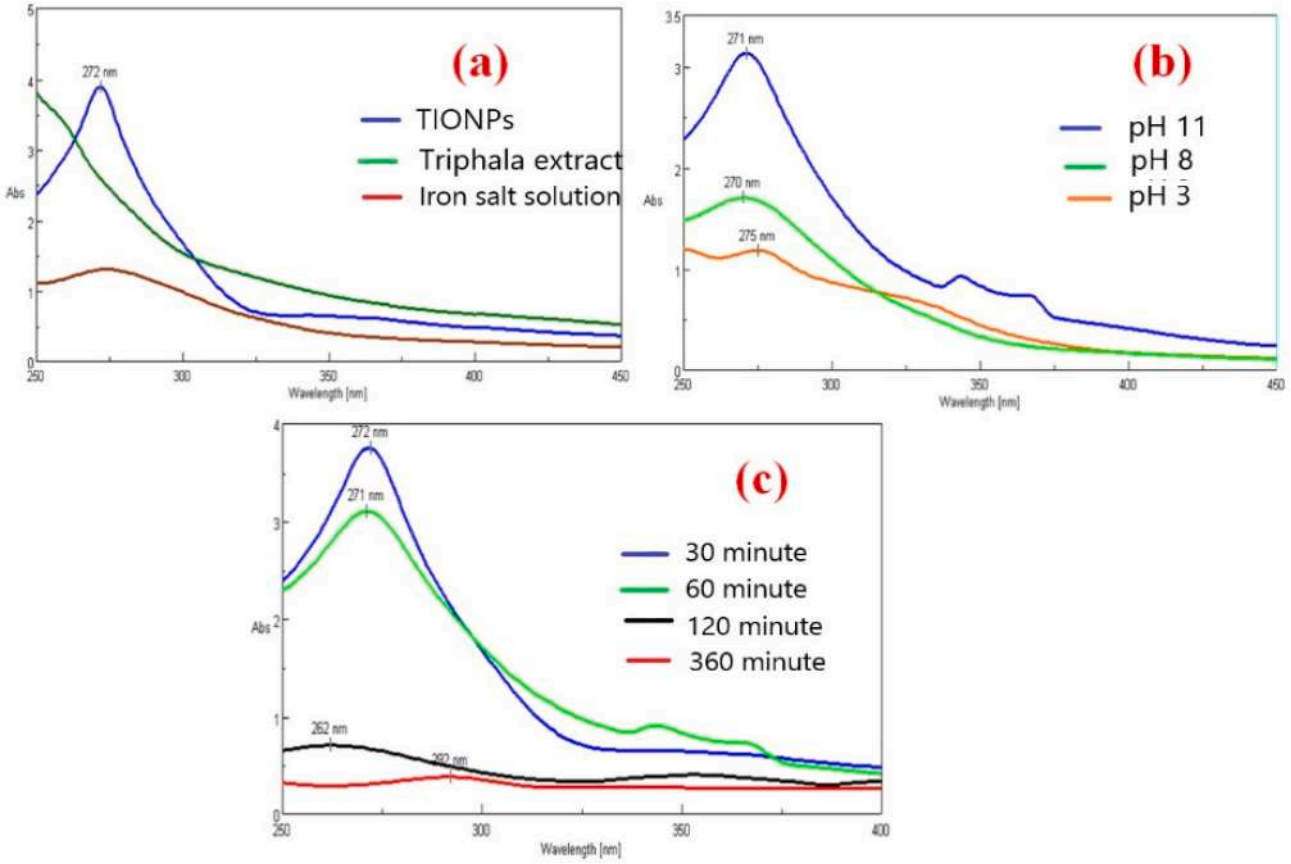

Fig. 3. UV–Visible spectrophotometer of TIONPs (a) Spectrum of $FeCl_3$ solution, triphala extract and TIONP suspension; (b) Comparative pH variant study; (c) Comparative time variant study.

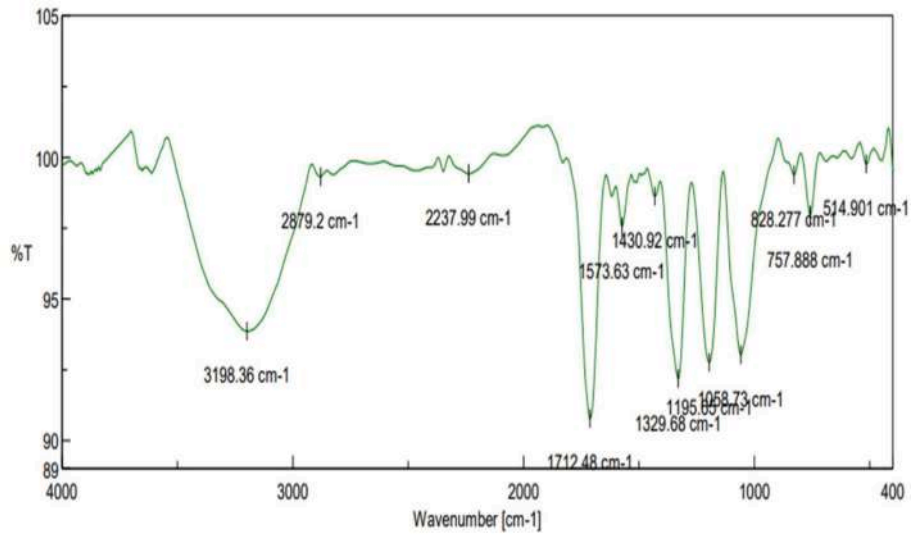

Fig. 4. FT-IR spectroscopy of TIONPs.

their potential in the treatment of breast cancer.

The free radical scavenging activity was evaluated by performing the DPPH assay method using ascorbic acid as standard reference. The IC_{50} value for ascorbic acid, Triphala extract and TIONPs were 7.693, 5.666 and 20.280 (μg/mL) respectively. The scavenging activity of aqueous extract of Triphala was found to be higher than that of the TIONPs due to the lower concentration of biomolecules in TIONPs suspension (Fig. 9A). Moreover, this observed free radical scavenging activity of TIONPs was found to be concentration dependent.

The in-vitro anti-inflammatory assay was done by protein denaturation method by using bovine serum albumin where diclofenac sodium as standard drug. The result revealed that the synthesized TIONPs were effective in inhibiting protein denaturation of albumin with 88.23% inhibition by the highest concentration (100 μg/mL) of the product (Fig. 9B). Interestingly, the TIONPs showed a better and significant anti-inflammatory activity than Triphala churna extract advocating the

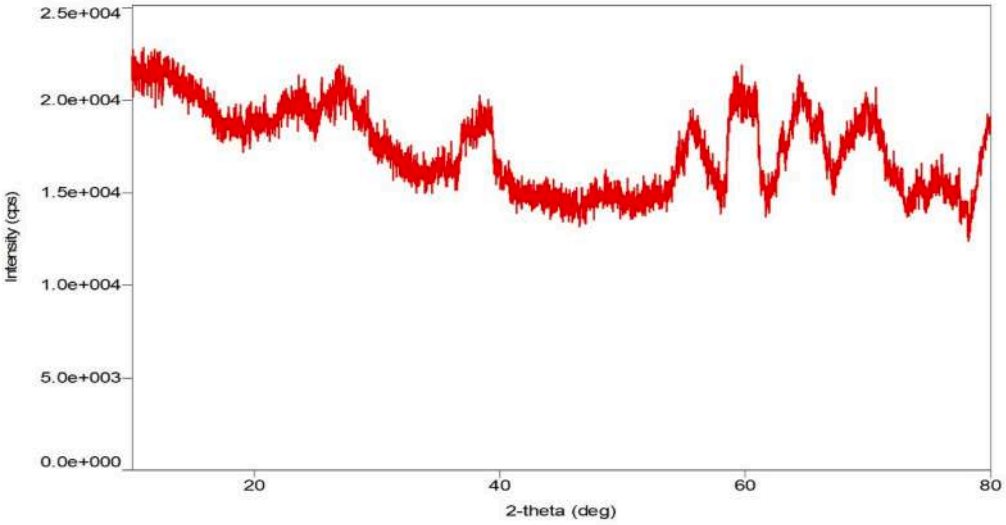

Fig. 5. X-Ray Diffraction pattern of synthesized TIONPs.

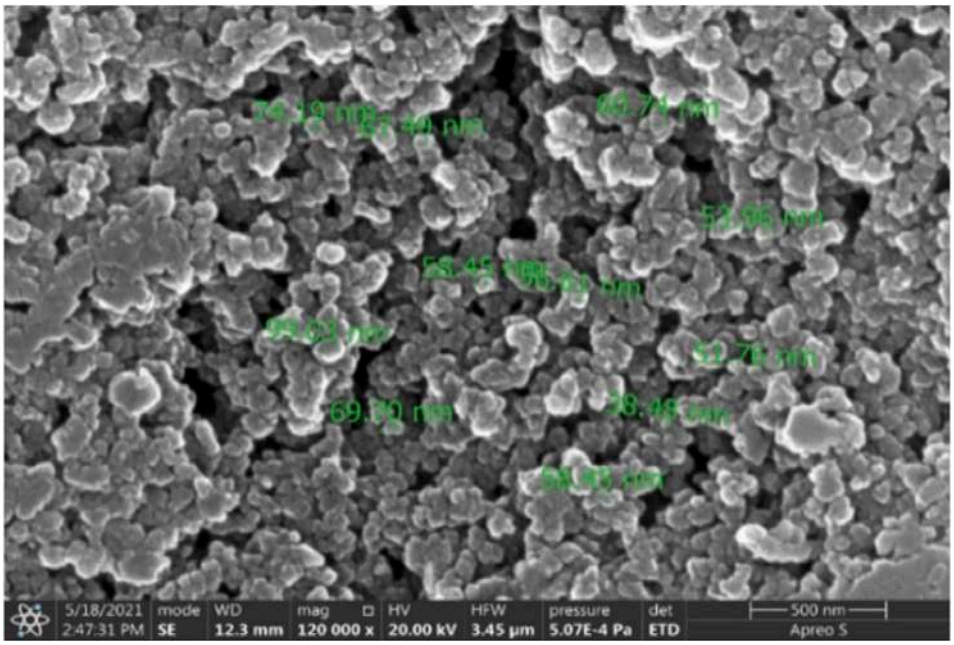

Fig. 6. SEM images of formulated TIONPs at scale bar of 500 nm.

advantage of administering this nano formulation over the conventional Ayurvedic churna. Our TIONPs having inherent antioxidant and anti-inflammatory activity is thus expected to stabilize and control the formation of excess free radicals to reduce the abnormal proliferation of breast cancer cells.

3.5. MTT assay

The secondary breast cancer leads to metastasis of skin due to the rapid growth of cancerous cells towards subcutaneous or squamous cell. From a case study, it was elucidated that the breast cancer can lead to skin cancer through skin of chest, scalp, neck, and abdomen or through the blood capillaries or lymphatic system [48]. Thus, in this research work the cytotoxic effect and efficacy of synthesized TIONPs was evaluated in two TNBC specific cell lines namely, MDA MB231 and 4T1, along with a skin cancer cell line (A431). A healthy cell line (HEK 293) was kept as control to assess the treatment selectivity and safety towards normal cells.

The MTT cell viability assay indicates the percentage of healthy and live cells in a sample to quantify the relative number of live and dead cell i.e., cell proliferation. It is a type of colorimetric assay which is used to quantify the number of metabolically active cells with the intensity of the colour produced. In general, the cell viability of cancerous cell in the MTT assay, should be less than that of control normal cell to ensure the cytotoxic effect of the anticancer drug [49]. In our study, the TIONPs sample showed lesser percentage of live cancerous cells in comparison to the control cell (HEK 293) which implies the cytotoxic potential of TIONPs towards TNBC and A431 cell. The test results are represented in Fig. 10 where the anticancer efficacy of Triphala churna mediated IONPs was expressed in terms of the concentration causing 50% decrease in cell viability (IC50, µg/mL). For MDA MB 231 cell lines, TIONPs showed % cell viability of 38.56 ± 4.53 and 35.56 ± 2.53 at concentration of 500 µg/mL in 24 h and 48 h respectively. For 4T1 cell lines it showed % cell viability of 35 ± 1.41 and 25.42 ± 1.84 at concentration 500 µg/mL in

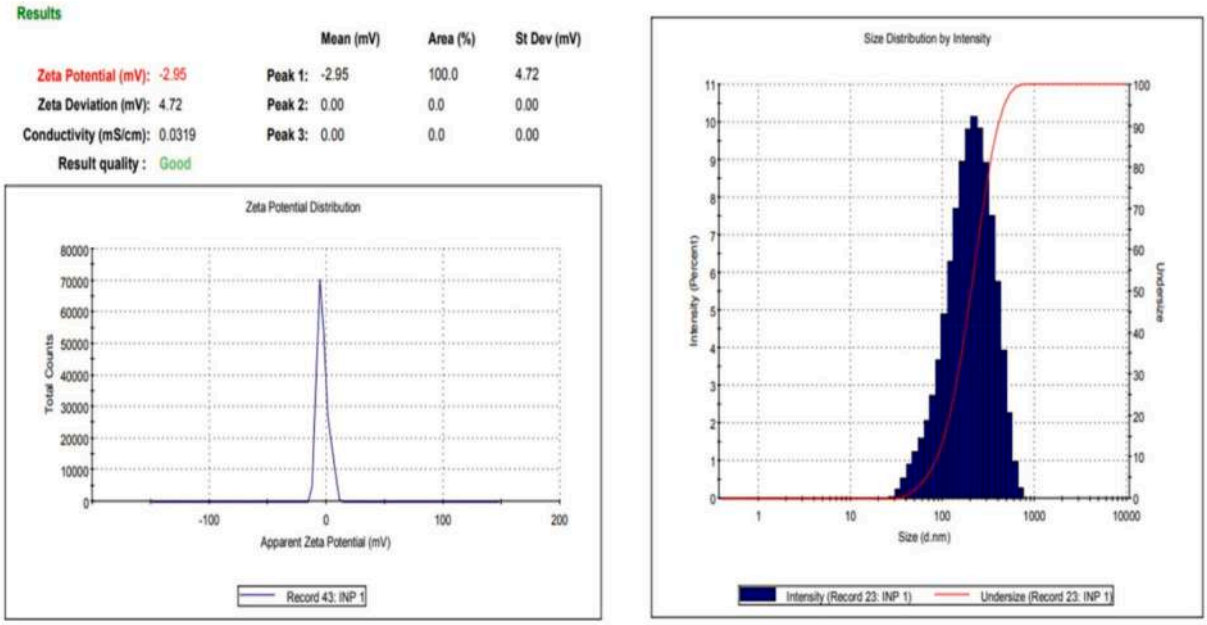

Fig. 7. DLS-Zeta potential analysis of synthesized TIONPs.

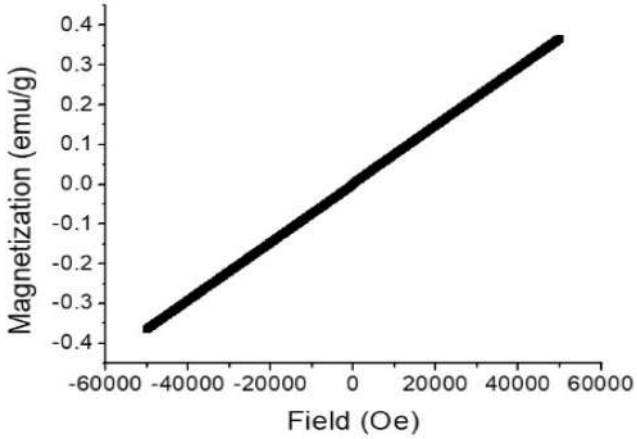

Fig. 8. Magnetic moment analysis of synthesized TIONPs by SQUID.

24 h and 48 h respectively. They also exerted 32 ± 1.47% cell viability at the 500 μg/mL concentration in 24 h and 25.24 ± 2.14% cell viability in 48 h for A431 cell lines. However, the non-cancerous (HEK) cell line showed much higher cell viability of 72 ± 1.58% and 54.30 ± 1.25% respectively at 500 μg/mL concentrations in 24 h and 48 h.

For both breast cancer (4T1, MDA MB 231) and skin cancer cell line (A431), a cell viability investigation revealed that the formulation (TIONPs) promoted greater cellular internalization and resulted in lower cell viability, indicating the cytotoxic nature of synthesized TIONPs towards cancer cell. The data also revealed that the said activity was concentration and time-dependant as the % of cell viability was gradually decreased with both concentration and time. The TIONPs were found to exert much less cytotoxic effect against the normal (host) cells in comparison to the cancerous cells, which advocate their use as potent anticancer agents in the future. Additionally, it is already observed that the IONPs are considered to be safe and nontoxic for human consumption as iron is a naturally occurring mineral in human body [50].

3.6. Nuclear staining assay

The nuclear staining assay is used as a support to MTT assay to investigate whether the test sample mediated cell death is induced by apoptosis or necrosis. The apoptosis indicates the programmed cell death without disturbing the normal function of the body. While, the necrosis is considered as the alternative to apoptosis where inappropriate or accidental cell death occurs by means of a toxic process. Thus, apoptosis is more preferable during cytotoxicity activity than necrosis to avoid the negative circumstances of immune system. The occurrence of apoptosis can be measured by nuclear staining assay by observing the morphological hallmarks like nucleus breakdown, collapsed chromatin fragmentation, nuclear envelope destruction and cell blebbing [51]. In our studies, the apoptotic cell population were observed by staining the nucleus using DAPI and AO after treatment with TIONPs. From the result it was confirmed that synthesized nanoparticles (TIONPs) induced maximum chromatin condensation, cell blebbing and cell shrinkage for MDA MB 231 cell lines. In case of the 4T1 and A431 cell lines, TIONPs treated cells induced more nuclear fragmentation and cytoplasmic shrinkage. AO penetrated both normal and dead cell and generated green fluorescence. Our study indicates that the viable cells show green fluorescence and the normal cells are characterized by the uniform chromatin with an intact cell membrane, whereas, nuclear fragmentation and membrane bubbles represents early apoptosis (Fig. 11). The late apoptosis cells exhibited white nuclei with condensed or fragmented chromatin. The results represented that the synthesized compound induced the majority of cell death through apoptosis mode indicating potent anticancer activity of TIONPs.

4. Conclusion

In the present study, Iron oxide nanoparticles have been synthesized from an aqueous extract of Triphala churna for the first time at a low cost and lesser time in a single-step process with enhanced antioxidant and cytotoxic activity. This synthesis did not utilize any harsh synthetic chemicals for the reduction of iron ions, instead it was carried out by green method using the reactive phytochemical groups of Triphala churna extract. The TIONPs showed promising cytotoxic activity against TNBC cells and associated skin cancer cell (A431), in comparison to the normal human cells. These TIONPs can be rapidly localized directly into the target organ utilizing their inherent paramagnetic property to reduce the side effects of current chemotherapeutic drugs. The green synthesized TIONPs can come up as a future anticancer drug for TNBC

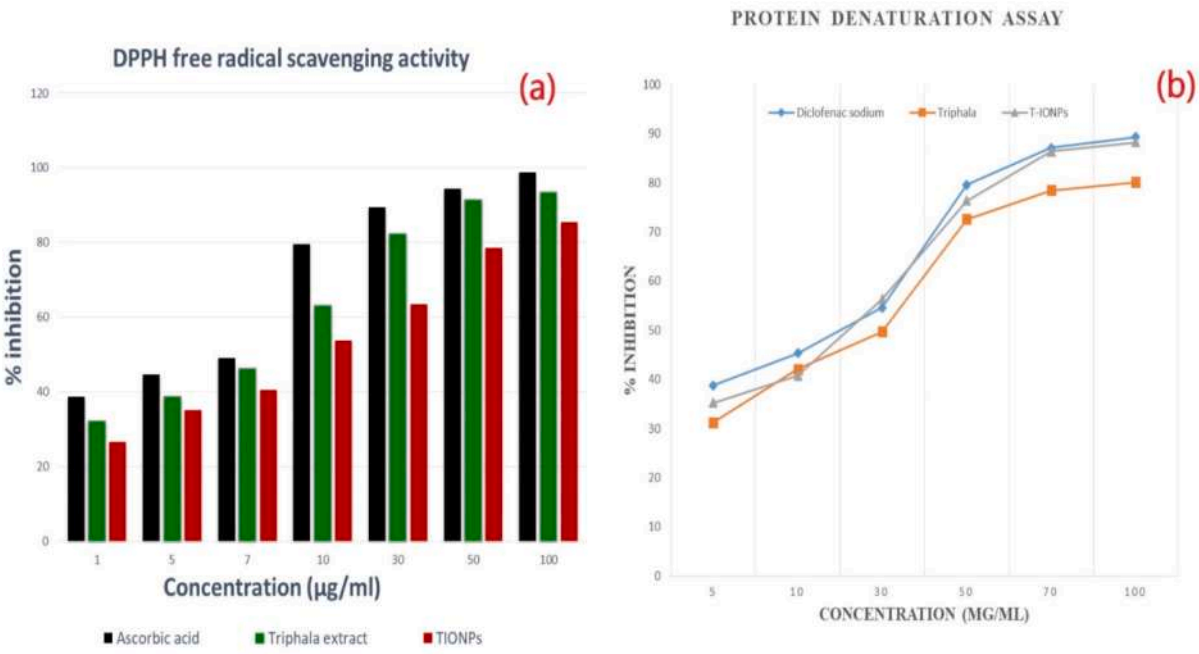

Fig. 9. Free radical scavenging activity of TIONPs by DPPH assay (a) In-vitro anti-inflammatory activity of TIONPs by protein denaturation assay (b).

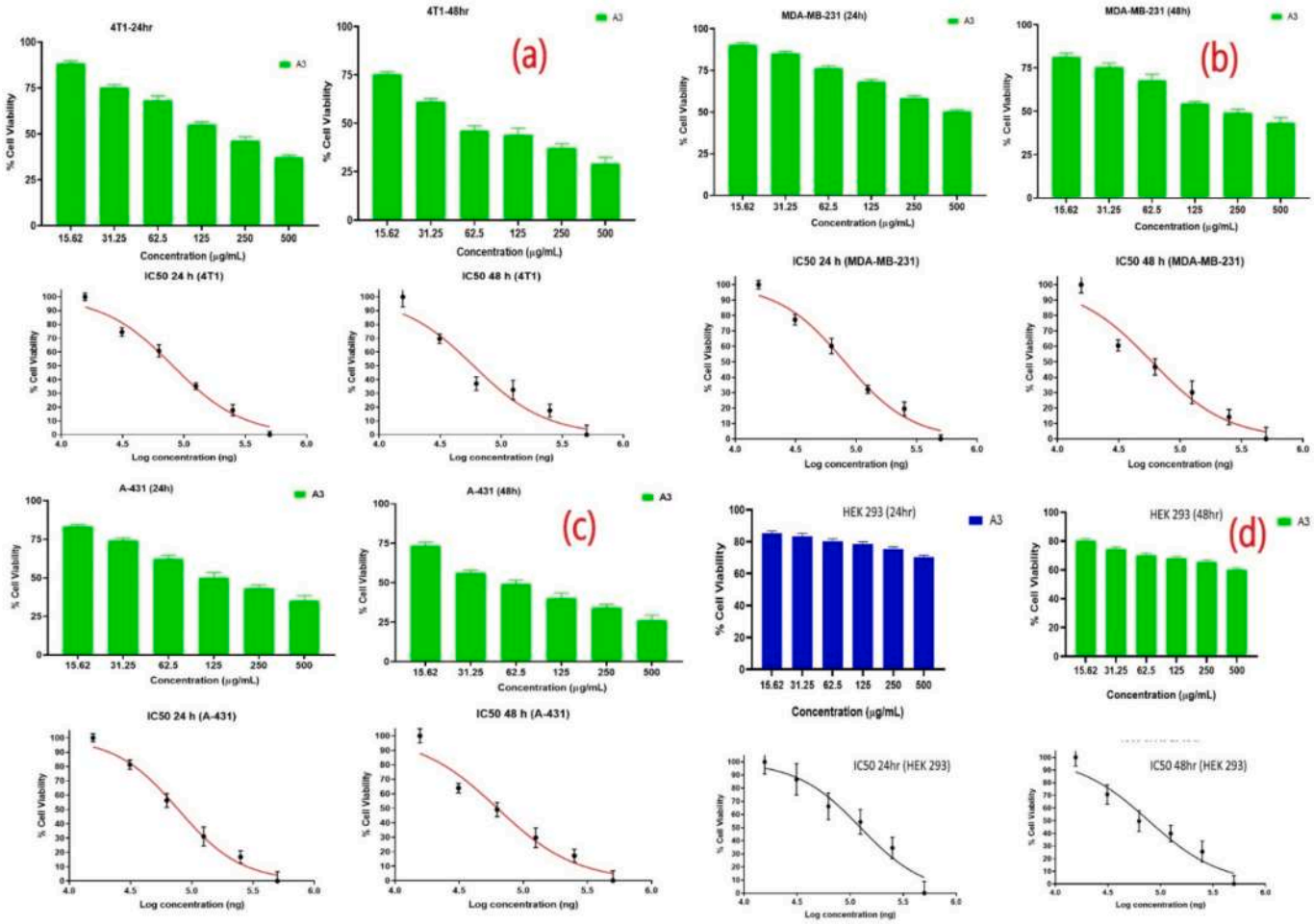

Fig. 10. In vitro cytotoxicity study of TIONPs **(a)** Cell viability study and IC_{50} value of 4T1 cells after treatment for 24 h and 48h **(b)** Cell viability study and IC_{50} value of MDA MB231 cells after treatment for 24 h and 48h **(c)** Cell viability study and IC_{50} value of A431 cells after treatment for 24 h and 48h **(d)** Cell viability study and IC_{50} value of HEK 293 cells after treatment for 24 h and 48h of HEK 293 cells.

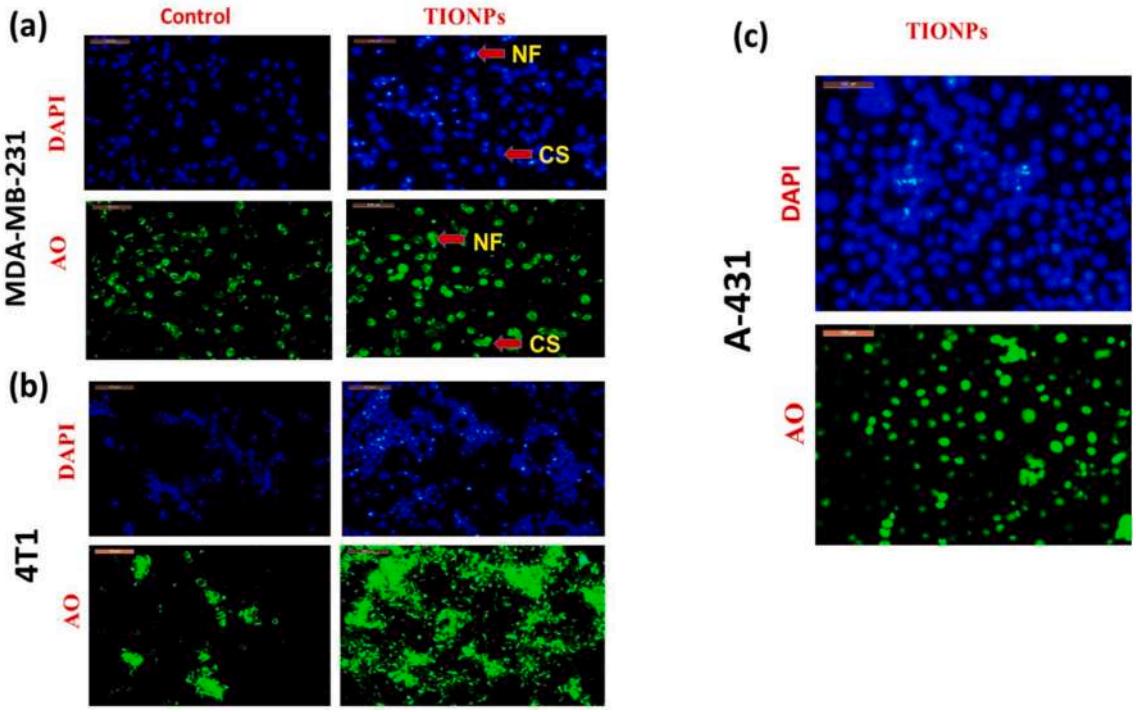

Fig. 11. Nuclear staining assay of TIONPs **(a)** MDA-MB-231 **(b)** 4T1 **(c)** A-431 cell lines.

treatment. However, extensive clinical studies are needed for confirming their safety and efficacy before commercialization.

Funding

This work has been supported by AICTE grant (File No. 8-65/FDC/RPS (POLICY-l)/2019-20) sanctioned to Prof. Anindya Bose under Research Promotion Scheme (RPS).

Author statement

Ankita Parmanik: Methodology; Investigation; Validation; Writing - original draft; Writing - review & editing.

Anindya Bose: Conceptualization; Methodology; Supervision; Writing - review & editing.

Bhavna Ghosh: Investigation, Writing - original draft.

Milan Paul: Investigation, Writing - original draft.

Asif Itoo: Investigation, Writing - original draft.

Swati Biswas: Methodology; Supervision; Writing - review & editing.

Manoranjan Arakha: Methodology; Supervision; Writing - review & editing.

Declaration of competing interest

The authors declare that they have no known competing financial interests or personal relationships that could have appeared to influence the work reported in this paper.

Data availability

Data will be made available on request.

Acknowledgements

We are thankful to the School of Pharmaceutical Sciences, Siksha O Anusandhan, Bhubaneswar, India and Birla Institute of Technology & Science-Pilani, Hyderabad Campus for providing necessary facilities for carrying out this research work. Additionally, we are also thankful to NISER, Bhubaneswar for providing the SQUID facility along with the technical help from Prof. Subhankar Bedanta and Dr. Sagarika Nayak in the SQUID measurement.

References

[1] L. Huang, X. Weng, Z. Chen, M. Megharaj, R. Naidu, Green synthesis of iron nanoparticles by various tea extracts: comparative study of the reactivity, Spectrochim. Acta Mol. Biomol. Spectrosc. 130 (2014 Sep 15) 295–301, https://doi.org/10.1016/j.saa.2014.04.037.

[2] L. Wilkinson, T. Gathani, Understanding breast cancer as a global health concern, Br. J. Radiol. 95 (1130) (2022 Feb 1), 20211033, https://doi.org/10.1259/bjr.20211033.

[3] T.C. de Ruijter, J. Veeck, J.P. de Hoon, M. van Engeland, V.C. Tjan-Heijnen, Characteristics of triple-negative breast cancer, J. Cancer Res. Clin. Oncol. 137 (2) (2011 Feb) 183–192, https://doi.org/10.3389/fonc.2021.710337.

[4] S.S. Shaikh, L.A. Emens, Current and emerging biologic therapies for triple negative breast cancer, Expet Opin. Biol. Ther. 22 (5) (2022 May 4) 591–602, https://doi.org/10.1080/14712598.2020.1801627.

[5] P. Chowdhury, U. Ghosh, K. Samanta, M. Jaggi, S.C. Chauhan, M.M. Yallapu, Bioactive nanotherapeutic trends to combat triple negative breast cancer, Bioact. Mater. 6 (10) (2021 Oct 1) 3269–3287, https://doi.org/10.1016/j.bioactmat.2021.02.037.

[6] R. Yadwade, S. Kirtiwar, B. Ankamwar, A review on green synthesis and applications of iron oxide nanoparticles, J. Nanosci. Nanotechnol. 21 (12) (2021 Dec 1) 5812–5834, https://doi.org/10.1166/jnn.2021.19285.

[7] K. Jiang, L. Zhang, G. Bao, Magnetic iron oxide nanoparticles for biomedical applications, Curr. Opin. Biomed. Eng. 20 (2021 Dec 1), 100330, https://doi.org/10.1016/j.cobme.2021.100330.

[8] World Health Organization, Cancer Control: Knowledge into Action: WHO Guide for Effective Programmes. Policy and Advocacy. Module vol. 6, World Health Organization, 2008.

[9] A.S. Thakor, S.S. Gambhir, Nanooncology: the future of cancer diagnosis and therapy, CA A Cancer J. Clin. 63 (6) (2013 Nov) 395–418, https://doi.org/10.3322/caac.21199.

[10] A.R. Bilia, M.C. Bergonzi, The G115 standardized ginseng extract: an example for safety, efficacy, and quality of an herbal medicine, J. Ginseng.Res 44 (2) (2020 Mar 1) 179–193, https://doi.org/10.1016/j.jgr.2019.06.003.

[11] E.S. Ong, Extraction methods and chemical standardization of botanicals and herbal preparations, J. Chromatogr. B 812 (1–2) (2004 Dec 5) 23–33, https://doi.org/10.1016/j.jchromb.2004.07.041.

[12] A. Shivakumar, S. Paramashivaiah, R.S. Anjaneya, J. Hussain, S. Ramachandran, Pharmacognostic evaluation of triphala herbs and establishment of chemical stability of triphala caplets, Int. J. Pharma Sci. Res. 7 (1) (2016 Jan 1) 244–251.

[13] N.S. Kumar, A.S. Nair, M. Murali, S.D. Ps, Qualitative phytochemical analysis of triphala extracts, J. Pharmacogn. Phytochem. 6 (3) (2017) 248–251.

[14] D.K. Kadam, P.D. Ahire, J.V. Bhoye, A.R. Patil, D.K. Yadav, Comparative standardization study of three Triphala churna formulation, Int J Pharmacogn (Panchkula, India)[Online] 4 (2) (2018) 71–78, https://doi.org/10.13040/IJPSR.0975-8232.IJP.3(11).482-90.
[15] S. Ahmed, X. Ding, A. Sharma, Exploring scientific validation of Triphala Rasayana in ayurveda as a source of rejuvenation for contemporary healthcare: an update, J. Ethnopharmacol. 273 (2021 Jun 12), 113829, https://doi.org/10.1016/j.jep.2021.113829.
[16] T. Sandhya, K.M. Lathika, B.N. Pandey, K.P. Mishra, Potential of traditional ayurvedic formulation, Triphala, as a novel anticancer drug, Cancer Lett. 231 (2) (2006 Jan 18) 206–214, https://doi.org/10.1016/j.canlet.2005.01.035.
[17] S. Cheriyamundath, T. Mahaddalkar, S.N. Save, S. Choudhary, R.V. Hosur, M. Lopus, Aqueous extract of Triphala inhibits cancer cell proliferation through perturbation of microtubule assembly dynamics, Biomed. Pharmacother. 98 (2018 Feb 1) 76–81, https://doi.org/10.1016/j.biopha.2017.12.022.
[18] S. Prasad, S.K. Srivastava, Oxidative stress and cancer: chemopreventive and therapeutic role of triphala, Antioxidants 9 (1) (2020 Jan) 72, https://doi.org/10.3390/antiox9010072.
[19] M.S. Murthy, Anticancer and pro-apoptotic effects of Triphala extract in human breast cancer MCF-7 cells, Faseb. J. 32 (2018 Apr) 151–152, https://doi.org/10.1096/fasebj.2018.32.1_supplement.151.2.
[20] S. Chakrapany, S. Chandan, Nano carriers of novel drug delivery system for 'ayurveda herbal remedies' need of hour–a bird's eye view, Am. J. PharmTech Res. 4 (2) (2014) 60–69.
[21] S. Ranjani, S. Hemalatha, Triphala decorated multipotent green nanoparticles and its applications, Mater. Lett. 308 (2022 Feb 1), 131184, https://doi.org/10.1016/j.matlet.2021.131184.
[22] E. Jayajothi, T. Elavarasu, M. Hamsaveni, S.K. Sridhar, Antioxidant activity and total phenolic content of triphala churna, Nat. Prod. Sci. 10 (1) (2004) 16–19.
[23] A. Khorasani Esmaeili, R. Mat Taha, S. Mohajer, B. Banisalam, Antioxidant activity and total phenolic and flavonoid content of various solvent extracts from in vivo and in vitro grown Trifolium pratense L.(Red Clover), BioMed Res. Int. 2015 (2015 Oct), https://doi.org/10.1155/2015/643285.
[24] S. Mukhi, A. Bose, A. Ray, P.K. Swain, Analytical standards of amrtadi churna: a classical ayurvedic formulation, Indian J. Pharmaceut. Sci. 79 (2) (2017 May 15) 227–240, https://doi.org/10.4172/pharmaceutical-sciences.1000221.
[25] R. Sood, D.S. Chopra, Improved yield of green synthesized crystalline silver nanoparticles with potential antioxidant activity, Int. Res. J. Pharm. 8 (4) (2017) 100–104, https://doi.org/10.7897/2230-8407.080457.
[26] A.S. Prasad, Iron oxide nanoparticles synthesized by controlled bio-precipitation using leaf extract of Garlic Vine (Mansoa alliacea), Mater. Sci. Semicond. Process. 53 (2016 Oct 1) 79–83, https://doi.org/10.1016/j.mssp.2016.06.009.
[27] J.A. Abdullah, L.S. Eddine, B. Abderrhmane, M. Alonso-González, A. Guerrero, A. Romero, Green synthesis and characterization of iron oxide nanoparticles by pheonix dactylifera leaf extract and evaluation of their antioxidant activity, Sustainable Chem.Pharm. 17 (2020 Sep 1), 100280, https://doi.org/10.1016/j.scp.2020.100280.
[28] K.D. Gunathilake, K.K. Ranaweera, H.P. Rupasinghe, In vitro anti-inflammatory properties of selected green leafy vegetables, Biomedicines 6 (4) (2018 Dec) 107, https://doi.org/10.3390/biomedicines6040107.
[29] P.G. Anantharaju, P.C. Gowda, M.G. Vimalambike, S.V. Madhunapantula, An overview on the role of dietary phenolics for the treatment of cancers, Nutr. J. 15 (1) (2016 Dec) 1–6, https://doi.org/10.1186/s12937-016-0217-2.
[30] Y. Cai, Q. Luo, M. Sun, H. Corke, Antioxidant activity and phenolic compounds of 112 traditional Chinese medicinal plants associated with anticancer, Life Sci. 74 (17) (2004 Mar 12) 2157–2184, https://doi.org/10.1016/j.lfs.2003.09.047.
[31] H. Sakakibara, Y. Honda, S. Nakagawa, H. Ashida, K. Kanazawa, Simultaneous determination of all polyphenols in vegetables, fruits, and teas, J. Agric. Food Chem. 51 (3) (2003 Jan 29) 571–581, https://doi.org/10.1021/jf020926l.
[32] E.C. Alegria, A.P. Ribeiro, M. Mendes, A.M. Ferraria, A.M. Do Rego, A.J. Pombeiro, Effect of phenolic compounds on the synthesis of gold nanoparticles and its catalytic activity in the reduction of nitro compounds, Nanomaterials 8 (5) (2018 May) 320, https://doi.org/10.3390/nano8050320.
[33] R.R. Pillai, P.B. Sreelekshmi, A.P. Meera, S. Thomas, Biosynthesized iron oxide nanoparticles: cytotoxic evaluation against human colorectal cancer cell lines, Mater. Today Proc. (2022 Jan 20), https://doi.org/10.1016/j.matpr.2022.01.151.
[34] D.A. Demirezen, Y.Ş. Yıldız, Ş. Yılmaz, D.D. Yılmaz, Green synthesis and characterization of iron oxide nanoparticles using Ficus carica (common fig) dried fruit extract, J. Biosci. Bioeng. 127 (2) (2019 Feb 1) 241–245, https://doi.org/10.1016/j.jbiosc.2018.07.024.
[35] L. Katata-Seru, T. Moremedi, O.S. Aremu, I. Bahadur, Green synthesis of iron nanoparticles using Moringa oleifera extracts and their applications: removal of nitrate from water and antibacterial activity against Escherichia coli, J. Mol. Liq. 256 (2018 Apr 15) 296–304, https://doi.org/10.1016/j.molliq.2017.11.093.
[36] M.S. Bhuiyan, M.Y. Miah, S.C. Paul, T.D. Aka, O. Saha, M.M. Rahaman, M.J. Sharif, O. Habiba, M. Ashaduzzaman, Green synthesis of iron oxide nanoparticle using Carica papaya leaf extract: application for photocatalytic degradation of remazol yellow RR dye and antibacterial activity, Heliyon 6 (8) (2020 Aug 1), e04603, https://doi.org/10.1016/j.heliyon.2020.e04603.
[37] H.R. Ali, H.N. Nassar, N.S. El-Gendy, Green synthesis of α-Fe2O3 using Citrus reticulum peels extract and water decontamination from different organic pollutants, Energy Sources, Part A Recovery, Util. Environ. Eff. 39 (13) (2017 Jul 3) 1425–1434, https://doi.org/10.1080/15567036.2017.1336818.
[38] M.V. Arularasu, J. Devakumar, T.V. Rajendran, An innovative approach for green synthesis of iron oxide nanoparticles: characterization and its photocatalytic activity, Polyhedron 156 (2018 Dec 1) 279–290, https://doi.org/10.1016/j.poly.2018.09.036.
[39] A. Gangopadhyay, R. Saha, A. Bose, R.N. Sahoo, S. Nandi, R. Swain, M. Paul, S. Biswas, R. Mohapatra, Effect of annealing time on the applicability of potato starch as an excipient for the fast disintegrating propranolol hydrochloride tablet, J. Drug Deliv. Sci. Technol. 67 (2022), 103002, https://doi.org/10.1016/j.jddst.2021.103002.
[40] Z. Cheng, A.L. Tan, Y. Tao, D. Shan, K.E. Ting, X.J. Yin, Synthesis and characterization of iron oxide nanoparticles and applications in the removal of heavy metals from industrial wastewater, Int. J. Photoenergy 2012 (2012 May), https://doi.org/10.1155/2012/608298.
[41] H.S. Devi, M.A. Boda, M.A. Shah, S. Parveen, A.H. Wani, Green synthesis of iron oxide nanoparticles using Platanus orientalis leaf extract for antifungal activity, Green Process. Synth. 8 (1) (2019 Jan 1) 38–45, https://doi.org/10.1515/gps-2017-0145.
[42] M. Singh, R. Kaur, R. Rajput, S. Agarwal, S. Kumar, M. Sharma, A. Sharma, Analysis of process and formulation variables on chitosan based losartan potassium nanoparticles: preparation, validation and in vitro release kinetics, Recent . Innovations.Chem. Eng.(Formerly Recent Patents on Chemical Engineering) 13 (1) (2020 Feb 1) 41–54.
[43] M. Danaei, M. Dehghankhold, S. Ataei, F. Hasanzadeh Davarani, R. Javanmard, A. Dokhani, S. Khorasani, M.R. Mozafari, Impact of particle size and polydispersity index on the clinical applications of lipidic nanocarrier systems, Pharmaceutics 10 (2) (2018 May 18) 57.
[44] L.S. Ardakani, V. Alimardani, A.M. Tamaddon, A.M. Amani, S. Taghizadeh, Green synthesis of iron-based nanoparticles using Chlorophytum comosum leaf extract: methyl orange dye degradation and antimicrobial properties, Heliyon 7 (2) (2021 Feb 1), e06159, https://doi.org/10.1016/j.heliyon.2021.e06159.
[45] N. Beheshtkhoo, M.A. Kouhbanani, A. Savardashtaki, A.M. Amani, S. Taghizadeh, Green synthesis of iron oxide nanoparticles by aqueous leaf extract of Daphne mezereum as a novel dye removing material, Appl. Phys. A 124 (5) (2018 May) 1–7. https://link.springer.com/article/10.1007%2Fs00339-018-1782-3.
[46] B. Choudhury, R. Kandimalla, R. Elancheran, R. Bharali, J. Kotoky, Garcinia morella fruit, a promising source of antioxidant and anti-inflammatory agents induces breast cancer cell death via triggering apoptotic pathway, Biomed. Pharmacother. 103 (2018 Jul 1) 562–573, https://doi.org/10.1016/j.biopha.2018.04.068.
[47] S. Reuter, S.C. Gupta, M.M. Chaturvedi, B.B. Aggarwal, Oxidative stress, inflammation, and cancer: how are they linked? Free Radic. Biol. Med. 49 (11) (2010 Dec 1) 1603–1616, https://doi.org/10.1016/j.freeradbiomed.2010.09.006.
[48] S. Adams, L. Kozhaya, F. Martiniuk, T.C. Meng, L. Chiriboga, L. Liebes, T. Hochman, N. Shuman, D. Axelrod, J. Speyer, Y. Novik, Topical TLR7 agonist imiquimod can induce immune-mediated rejection of skin metastases in patients with breast cancer, Clin. Cancer Res. 18 (24) (2012 Dec 15) 6748–6757, https://doi.org/10.1158/1078-0432.CCR-12-1149.
[49] A. Bahuguna, I. Khan, V.K. Bajpai, S.C. Kang, MTT assay to evaluate the cytotoxic potential of a drug. ||| Bangladesh, J. Pharmacol. 12 (2) (2017 Apr 8) 115–118.
[50] A. Parmanik, A. Bose, B. Ghosh, Research advancement on magnetic iron oxide nanoparticles and their potential biomedical applications, Minerva.Biotechnol. Biomol. Res. 34 (2) (2022 Jun 1) 86–95, https://doi.org/10.23736/S2724-542X.21.02830-3.
[51] S. Elmore, Apoptosis: a review of programmed cell death, Toxicol. Pathol. 35 (4) (2007 Jun) 495–516, https://doi.org/10.1080/01926230701320337.

Online version at http://www.minervamedica.it

Minerva Biotechnology and Biomolecular Research 2022 mese;33(0):000–000
DOI: 10.23736/S2724-542X.21.02830-3

REVIEW

Research advancement on magnetic iron oxide nanoparticles and their potential biomedical applications

Ankita PARMANIK, Anindya BOSE *, Bhavna GHOSH

Department of Pharmaceutical Analysis, School of Pharmaceutical Sciences, Siksha 'O' Anusandhan (Deemed to be University), Bhubaneswar, India

*Corresponding author: Anindya Bose, School of Pharmaceutical Sciences, Siksha 'O' Anusandhan (Deemed to be University), Bhubaneswar, India.
E-mail: anindyabose_in@yahoo.com

ABSTRACT

Magnetic iron oxide nanoparticles (MIONPs) have turned into a big research hotspot in biomedical fields mostly due to their large surface area to volume ratio and inherent superparamagnetism property. Various physical and chemical methods have been developed for their synthesis such as coprecipitation, solvothermal reduction, thermal decomposition, electrochemical synthesis, etc. Although most of these methods suffer from operational hurdles as well as environmental hazards. Therefore research focus is now concentrating towards their synthesis from various biological or green resources like plant extracts, micro-organisms, algae, glucose, starch, clays, etc. Plant extracts are mostly acceptable for such type of green synthesis due to their ability to reduce iron ions rapidly as well as their easy availability in wide varieties. Magnetic iron oxide nanoparticles have been applied in various biomedical fields such as targeted localization, magnetic hyperthermia, magnetic resonance imaging, and nuclear magnetic resonance imaging, Bio-separation and sensing method, cancer detection/diagnosis, and many more applications. This review comprehensively depicts the methods and challenges in the preparation of magnetic iron oxide nanoparticles as well as their potential application in biomedical fields.

(*Cite this article as*: Parmanik A, Bose A, Ghosh B. Research advancement on magnetic iron oxide nanoparticles and their potential biomedical applications. Minerva Biotechnol Biomol Res 2022;33:000-000. DOI: 10.23736/S2724-542X.21.02830-3)

KEY WORDS: Biomedical technology; Magnetic iron oxide nanoparticles; Drug delivery systems.

Nanoparticles (NPs) are entities typically having a diameter from 1 to 100 nm. Their large surface area to volume ratio empowers them with many advantages for their biomedical applications like lower sedimentation rate, better tissular diffusion, improved bioavailability, high mechanical, thermal stability, etc. In addition, their surface modification can generate materials having desired biological, chemical, and physical properties that make them suitable for specific biological applications.[1]

Magnetic iron oxide nanoparticles (MIONPs) are gaining popularity in various biomedical fields due to their effective size control phenomena, surface characterization along with inherent superparamagnetism property. Their application spectrum includes magnetic resonance imaging (MRI), magnetic particle imaging, biosensing, targeted drug delivery as well as controlled release, in vivo imaging, antimicrobial activities, and many more.[1, 2] Various physical and chemical methods have been developed for the synthesis of MIONPs such as coprecipitation, solvothermal reduction, thermal decomposition, electrochemical synthesis, etc. These methods however suffer from different operational and environmental drawbacks; therefore researchers are now switching to the green routes of their synthesis. MIONPs possess many unique features (Figure 1) like size and shape-controlled properties, surface structure, increased stability, high magnetic response, and most importantly the potentiality to target a specific site for drug delivery.[2] Currently, they have high demand in bio-clinical and diagnostic fields, magnetic bioseparation, evaluation of biological materials like proteins, nucleic acids, enzymes, cells, etc. MIONPs prepared using safe and non-immunogenic materials can effortlessly pass through

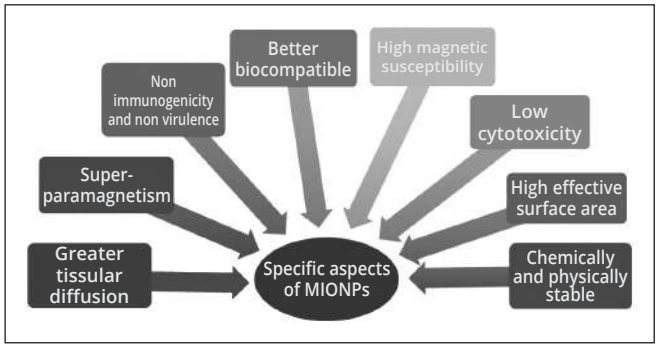

Figure 1.—Unique features of magnetic iron oxide nanoparticles.

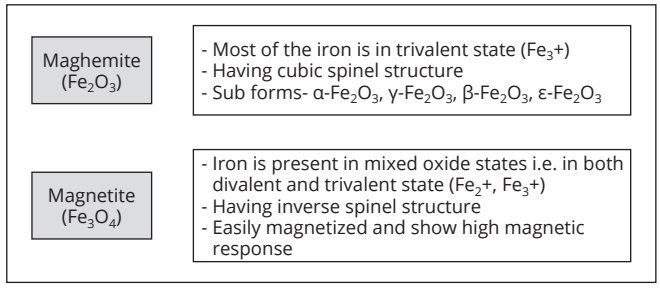

Figure 2—Iron oxide forms in MIONPs: maghemite *vs.* magnetite.

blood capillary systems to avoid vessel embolism. They also possess high magnetization to control their movement in blood effectively.[3] The main aim of this review is to describe the advancements made in the field of MIONPs synthesis with special on green synthesis, their biomedical applications as well as future prospects.

Magnetic nanoparticles can be eventually distinguished based on their oxidation state, surface attributes, and physicochemical properties, and most importantly by magnetism property. Oxide forms of magnetic nanoparticles have been most extensively used and explored. They are more sensitive, reactive, and stable than their native metallic nanoparticle verities. MIONPs have gained much more attention in comparison with other metal oxide magnetic nanoparticles, like copper and nickel, as these are highly toxic and prone to degradation. In contrast, MIONPs can be readily produced and possess excellent dimensional stability with a high magnetic response. They exhibit great potential in biomedical fields through their unique size, shape, stability, and dispersibility.

Iron oxides exhibit in many forms like Maghemite (γ-Fe_2O_3), Magnetite (Fe_3O_4), Hematite (α-Fe_2O_3, weakly ferromagnetic), Wusite (FeO, antiferromagnetic), Goethite (FeOOH, antiferromagnetic) and Epsilon phase magnetic iron oxide (ε-Fe_2O_3), etc. However, Maghemite and Magnetite with excellent inimitable superparamagnetism properties are mostly used in MIONPs (Figure 2).[3] Magnetite (Fe_3O_4) is a very common naturally occurring mineral with an inverse spinel structure. It is considered as the strongest magnetic material that can be easily manipulated for nanoparticle synthesis. Magnetite nanoparticles with low Curie temperature (850K), containing divalent iron to act as an electron donor, can remain ferromagnetic at room temperature. These particles do not retain any residual magnetism after removal of the external field; which helps them to avoid coagulation.[4]

Magnetic behavior

Magnetic behavior is the most significant characteristic of MIONPs which facilitates their biomedical applications. Particle size plays a crucial role in the manifestation of their superparamagnetism, high saturation field, and high irreversibility. It is reported that, when the sample size of multiple domain ferromagnetic particles is reduced to less than 30 nm, the magnetic spin is distorted resulting in the generation of a single domain structure having super-paramagnetic properties.[5] Iron oxide nanoparticles with a size range of 2-40 nm, called ultra-small superparamagnetic iron oxide nanoparticles (USPIONS), have more consequential importance in the biomedical field due to their distinctive magnetic property. Size reduction to nano-scale yields a single magnetic domain structure which empowers them with paramagnetic properties.

The larger surface-to-volume ratio of MIONPs generates high surface energy that can lead to their aggregation to reduce this energy. MIONPs should therefore be encapsulated with a biocompatible polymer during or after synthesis to avoid their aggregation and biodegradation. The large external magnetic field is desirable for their biomedical application especially in the diagnosis and detection of various types of tumors. It also allows more effective drug loading to the tumor site under the influence of a magnetic field. These super-paramagnetic nanoparticles exhibit their magnetic behavior only in the presence of the external magnetic field. This reduces the risk for their agglomeration and coagulation inside blood capillaries during biomedical applications.[6]

Approaches for the synthesis of MIONPs

Researchers are developing different novel methods for the preparation of MIONPs which majorly affect their particle size distribution, shape, crystallinity, magnetic properties, polydispersity, surface chemistry, and type of application.

Some indispensable parameters such as temperature, pH, concentration, stirring time, centrifugation speed, and duration of drying are needed to be monitored and optimized to achieve desired properties for these nanoparticles before, during, and after synthesis.[7]

Some important physical and chemical methods of MIONPs synthesis are listed in Supplementary Digital Material 1 (Supplementary Table I).[8-15] These methods can produce a large number of nanoparticles in a shorter time, but they most utilize environmentally hazardous chemicals. The major focus in MIONPs synthesis is therefore shifting towards the green synthesis of MIONPs due to their simplicity, biocompatibility, and safety aspects.

Green synthesis of MIONPs

The synthesis of nanoparticles from disparate biological sources is considered as "green synthesis" where the term 'green' itself indicates the safety of the environment. This method neither uses any hazardous chemicals nor produces any toxic byproducts for the successful implementation in various biomedical applications. The active phytoconstituents from different biological sources act both as reducing and capping agents to stabilize the nanoparticles and eliminates the need for any external chemical reagents.[4] The features and advantages of green methods of MIONPs synthesis are summarized in Figure 3.

Plant extracts are the most preferred biological source for the green synthesis of MIONPs, due to their high availability in bewildering varieties with diverse bioactive phytoconstituents to uplift the production. In comparison to plant extracts, the microorganisms like bacteria, fungi demand a lengthy incubation period for the synthesis. Researchers have also efficiently utilized other biological sources for their synthesis including carbohydrate, starch, glucose, amino acids, microorganisms, etc. However, the distinct type and characteristics of synthesized nanoparticles depend upon the source and the nature of the phytochemicals present in them.[16] Some significant examples of MIONPs synthesis through plant extracts and other biological sources are provided in Supplementary Digital Material 2 (Supplementary Table II, Supplementary Table III).[17-45]

Figure 3.—Advantages of green synthesis of MIONPs.

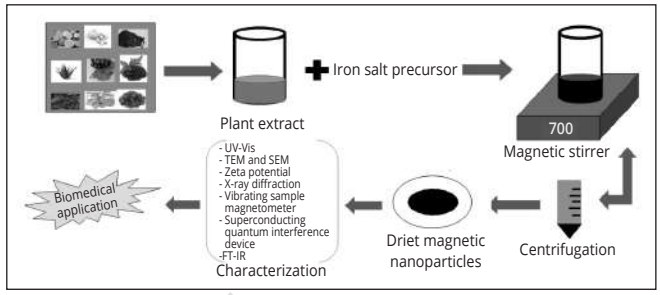

Figure 4.—Steps of green synthesis of MIONPs using plant extracts.

Figure 4 schematically depicts the steps for the plant extract mediated green synthesis of MIONPs. In brief, the required amount of iron salt solution is added to the plant extract and kept in a magnetic stirrer for proper mixing to prevent agglomeration. After completion of synthesis, when the medium turns to brownish-black color, is subjected to centrifugation followed by drying. After a predefined time, the dried mass of MIONPs is collected for further characterization followed by effective biomedical applications. The phytoconstituents like polyphenols, flavonoids, terpenoids, and sugars contents are primarily responsible for the bio-reduction of iron ions from Fe (II) to Fe (0) to form MIONPs. The success of the reaction and the nature of the nanoparticles produced depend on various factors like selection of plant sources, choice of the solvent medium (aqueous or non-aqueous), preparation of the iron salt solution, the ratio of the plant extract and salt solution, magnetic stirring speed, reaction parameters such as time, temperature, pH, stabilizing agent (if needed), centrifugation speed, etc.

Factors influencing the green synthesis of MIONPs

The successful synthesis of magnetic nanoparticles is challenging as several processing factors like tem-

perature, pH, iron salt concentration, stirring speed, reaction time, etc. portray crucial roles in the properties of MIONPs including particle size and shape, purity, crystallinity, and stability In plant-extract mediated synthesis, the choice of plant material is considered to be important as the presence of specific phytoconstituent classes like flavonoids, terpenoids, phenols, sugars, amino acids contribute significantly in the rapid reduction of the iron ions. Likewise, in microbial-mediated synthesis, the reaction is dependent upon the secretion of the microbial enzyme and the duration of agitation. Some dominant factors that substantially influence their quality (majorly the morphological features) are summarized below.

Particle size

The particle size plays an important role in determining the properties of MIONPs, most importantly their magnetism and surface area. When the size of nanoparticles is reduced to nano range, their melting point also reduces. Nanoparticles below 100 nm size exhibit greater colloidal stability in the aqueous medium (pH 7) with subsequent enhancement in their biological activities. It can be further stated that the most desirable size range of MIONPs for intravenous administration is 10-50 nm (already mentioned as USPIONS). This fact can be explained by the fact that particles greater than 50 nm size are captured by the liver and spleen cells and have higher chances of agglomeration. On the other hand, particles smaller than 10 nm are rapidly eliminated by the kidneys with subsequent shortening in their elimination half-life.[46]

Time

The reaction duration as well as heating time (if required) can also play a significant role in determining the size, shape, and magnetic properties of MIONPs. Longer synthesis time may lead to particle agglomeration and formation of clusters that result in enlarged particles with reduced stability.[47]

Temperature

The reaction temperature can be optimized only by trial and error as every green material contains a different set of phytoconstituents with a requirement of separate conditions for synthesis. Different shapes of the nanoparticle can be obtained by adjusting the temperature of the reaction mixture.[48] In a relevant research work, Rath *et al.* (2019) biosynthesized semi-spherical shaped MIONPs (25-55 nm) using the leaf extract of pomegranate seeds and 1M iron chloride solution at 70 °C. They observed that maintenance of high temperature resulted in the formation of hematite nanoparticles.[27] Suganya *et al.* (2016) during the biosynthesis of iron oxide nanoparticles from *Passiflora foetida* leaf extract at 60±1 °C temperature reported spherical shaped particles of 10-16nm sizes through SEM imaging.[37]

pH

The crystallinity of nanoparticles is regulated by the nucleation and growth mechanism, where the atoms or molecules are assembled directly to form clusters. In the case of green synthesis of MIONPs, the pH of the reaction medium is dependent on the phytoconstituents of the plant extract used. It is reported that the pH of the medium can affect the rate of synthesis, crystal growth of nuclei, and the morphology of the final product due to the nucleation effect; where the nuclei act as a carrier for crystal growth.[49] The pH of the medium also influences the rate of reduction of the metal ions.[47] In one such relevant research work, Saranya *et al.* (2017) demonstrate the effect of pH on the green synthesized MIONPs prepared from the mixture of *Musa ornata* flower sheath extract and Ferrous sulfate solution. They found that pH has a major impact on the size and dissolution of nanoparticles with synthesis seemed to be faster in alkaline medium.[23]

Storage condition

Storage conditions may vary according to the nature of nanoparticles formed. Some MIONPs require dry condition while others need cool storage.[50] The nature of the phytoconstituents present in the plant extracts may be critical in selecting a specific storage condition, as their degradation may lead to unsuccessful synthesis or instability of the produced MIONPs. Generally, 4 °C is preferred for the long-term storage.[50]

Other factors

The stirring speed during synthesis can be manipulated to effectively control the size and shape of nanoparticles. The metal reduction process occurs faster at ambient pressure during the synthesis of MIONPs. After complete synthesis, the particles are separated from the solution by centrifugation process at an optimum centrifugation speed to achieve the desired size of nanoparticles.[46, 50]

The characteristics and quality of the nanoparticle may get affected by the relative concentration of the precursor

solution and biological extract.[51] Additionally, the variation in the composition of phytoconstituents and the nature of the plant source can ultimately determine the quality and quantity of the nanoparticles produced. Efficient separation of synthesized nanoparticles is very crucial in their green synthesis process; as otherwise extra-biological materials and impurities may interfere with their biological activities.[52]

Characterization techniques

MIONP evaluation methods assure their size and size distribution, shape, porosity, aggregation, zeta potential, surface chemistry, crystallinity, colloidal stability, magnetic property, etc. Various analytical techniques are employed to estimate their properties including Ultraviolet-Visible spectroscopy (UV-Vis), Fourier transforms Infra-red spectroscopy (FT-IR), X-Ray diffraction (XRD), Atomic force microscopy (AFM), X-ray photoelectron spectroscopy (XPS), Thermo-gravimetric analysis (TGA), Nuclear magnetic resonance (NMR), Scanning electron microscope (SEM), Transmission Electron Microscopy (TEM), Nanoparticle tracking analysis (NTA), Dynamic light scattering (DLS), etc. Although, selecting a proper set of characterization techniques remains the most important task and should be decided based on the desired application.

The morphology and size distribution of nanoparticles can be characterized by SEM, TEM, DLS, Zeta Potential Analyzer (zetasizer), etc. Atomic force microscopy, an ultra-high-resolution tool, can be typically used for the evaluation of quantitative information like length, width, height, the surface texture of individual as well as grouped nanoparticles. Nanoparticle tracking analysis visualizes and measures suspended nanoparticles in the 10-1000 nm range based on the principle of Brownian motion. XPS is used productively for the determination of reaction mechanisms nanoparticles with the study of surface chemistry. The apparent confirmation of the binding efficiency of the polymer on the surface of magnetic nanoparticles can be done by TGA. Some rapid and sensitive chromatographic techniques such as size exclusion chromatography (SEC), Hydrodynamic chromatography (HDC), Field flow fractionation (FFF) are efficiently performed to separate the nanoparticles based on their size, hydrodynamic radius, and surface texture, etc. Some primary analytical techniques used to establish the physicochemical characteristic of MIONPs are listed in Table I.[7, 37]

TABLE I.—*Major techniques for MIONP characterization.*

Technique	Utility
Scanning electron microscope (SEM)	• Particle size • Particle shapes (*e.g.*, spherical, rod, irregular, etc.) • Crystallinity
Transmission Electron Microscopy (TEM)	• Morphological features (size, shape, and size distribution). • Particle size and clusters
Zeta potential	• Stability of colloidal solution • Measurement of electrostatic potential
Fourier-Transform Infrared Spectroscopy (FT-IR)	• Functional groups and nature of attached biomolecules • Data on light absorption, emission, raman scattering, and vibrational energy.
X-Ray Diffraction (XRD)	• Crystallinity • Elemental composition
Ultraviolet-Visible Spectroscopy (UV-Vis)	• Absorption spectra and reaction progress
Small Angle X-ray Scattering	• Nanoscale density • Size, shape, and the pore size
Vibrating Sample Magnetometer (VSM)	• Magnetic moment • Magnetism behavior
Superconducting Quantum Interference Devices (SQUID)	• Output voltage (Flux profile) • Magnetic property

Biomedical applications

In recent years, there is a remarkable increase in the application of MIONPs in Biomedical fields. They have gained considerable attention in targeted localization, magnetic hyperthermia, MRI and NMR imaging, bioseparation and sensing method, cancer detection, diagnosis any many more applications.[10] Uncapped iron oxide nanoparticles suffer the limitation of being highly reactive and prone to oxidation which may lead to damage to their magnetic behavior as well as dispersion. They are therefore generally coated with silica, phospholipids, organic fatty acids, and other inorganic materials to ensure their stability and biocompatibility. Some of their significant biomedical applications are described below.

Targeted drug delivery

Targeted drug delivery systems are designed to carry drug molecules directly into a specific region of the body. This helps to reduce their dose of administration and thereby toxic effects. In the case of MIONP based targeted drug delivery, the inherent magnetic properties of MIONPs are utilized by an exogenous magnetic field to regulate their movement towards the desired targeted site of the body. After injection of the MIONP based drug delivery systems,

drug molecules move through the systemic circulation through capillary systems without vessel embolism. As the drug is transported to a specific target site, the chances of side effects and dosage requirements are reduced.[53-55] Some notable works in this field are mentioned in Supplementary Digital Material 3 (Supplementary Table IV).[54-63]

Magnetic hyperthermia

Magnetic hyperthermia (thermotherapy) is a type of therapy where cancer tissue is exposed to high temperatures that kills them with minimum injury to surrounding normal healthy cells. Magnetic hyperthermia alters the cellular homeostasis of cancerous cells by protein denaturation which results in dysfunctioning of the cell cycle. Protein synthesis and DNA repairing are inactivated by the production of reactive oxygen species which ultimately damages their nuclear protein. This leads to inhibition of cell proliferation resulting in the death of tumor cells.

Superparamagnetic iron oxide nanoparticles (SPIONS) are the most extensively tested magnetic mediators in these applications. MIONPs are administered intravenously and get accumulated in tumors to induce heat using an externally delivered transducing energy. Three important mechanisms considered for heat generation are:[64]

- eddy current (induction effect);
- frictional heating (Generated by the interaction between MIONPs and surrounding medium);
- neel or BROWNIAN RELAXATION (Loss of Hysteresis loops of MIONPs).

Some examples of the application of Magnetic hyperthermia are provided in Supplementary Digital Material 4 (Supplementary Table V).[65-74]

MRI

MRI is considered to be a noninvasive bio-imaging technique producing high-resolution images of internal organs of the body. As a diagnostic tool, MRI provides high spatial resolution images of the anatomical structure of the tissue. MIONPs have some excellent physicochemical properties which make them suitable as a contrasting agent in MRI. These include: 1) strong and tunable magnetic response; 2) enhanced pharmacokinetic properties with longer retention time in blood and tissue; and 3) assorted surface phenomena for multimodal bioimaging.[75] MIONPs greater than 10 nm size have been employed as negative contrast while particles smaller than 5 nm are suitable as positive contrast in early detection of the malignant tumors. In these applications, core-shell nanoparticles are generally used as contrast agents to achieve lower retention time and improved biocompatibility for greater safety.[76, 77] Some examples of MRI applications of MIONPs are given in Supplementary Digital Material 5 (Supplementary Table VI).[78-86]

SPIONs have been used in clinical imaging for more than two decades. However, many SPIONs are recently taken off the market due to their limited spectrum of applications as well as concern about impaired mitochondrial function, the appearance of apoptotic bodies, the generation of free radicals, and DNA damage.[46, 77] Currently, there is an emerging trend to replace SPIONs with ultra-small superparamagnetic iron oxide nanoparticles (USPIONs) with a mean hydrodynamic diameter lesser than 50 nm. USPIOs have a comparatively longer half-life in systemic circulation and therefore have a wider spectrum of applications. However, they should be cautiously used to prevent their possible immune responses. Several strategies have been proposed for this including aspirin intake prior to USPIO administration to inhibit complement activation and prevent hemodynamic reactions to liposomes. Similar administration of low-molecular-weight dextrans has also been fruitful by blocking the circulating antidextran antibodies. The green synthesis of IONPs can easily be manipulated to USPIONs by altering the different parameters such as concentration of salt and ratio of the green extract with precursor solution, temperature, pH, etc. Surface modifications of IONPs with biocompatible biopolymers can further minimize the chances of agglomeration.[46]

Miscellaneous applications

MIONPs based biosensors with different sizes, shapes, and magnetic properties are used to identify specific molecular targets. Superparamagnetic Iron oxide nanoparticles (SPIONS) are capable of magnetic field aided transportation of biomaterials in a very fast, efficient, and reliable manner.[87] They have been able to separate and purify some specific biological entities like proteins, DNA fragments, etc. SPIONs also has tremendous potential in the early detection and screening of malignant tumors by targeting specific tumor cell receptors.

Superparamagnetic relaxometry (SPMR), a novel and advanced tool, utilizes highly sensitive magnetic biosensors conjugated superparamagnetic iron oxide nanoparticles for the effective detection of cancers. SPMR possesses desirable sensitivity and specificity to measure the cell numbers within a tumor.[88] Nanoparticles with a specific

size range are needed in these cases for the formation of mono-dispersed MIONPs with high magnetic properties. Accordingly, Superconducting Quantum Interference Devices (SQUID) have been developed as a detector to trace and quantify the magnetization of malignant tumor bound SPIONS.[87, 88]

Green synthesized MIONPs have also been found to be effective in other important treatment fields (Supplementary Digital Material 6: Supplementary Table VII)[89-99] like antibacterial/antimicrobial treatment, cancer therapy, free radical scavenging (Antioxidant), etc. MIONPs have been reported to be efficient in the localized delivery of plant extracts within human body systems. Tuzun *et al.* (2020) have reported the antioxidant, cytotoxic effects of MIONPs prepared from the extract of *Asphodelus aestivus*. They reported that MIONPs was highly effective in treating breast cancer and melanoma cell lines by alteration of the gene expression responsible for the cancer prognosis.[88]

Conclusions

MIONPs are considered to be biocompatible and safe for human consumption as iron being a naturally occurring metal of the human body. They can be regulated by a magnetic field, thereby improving their recovery, activity, and stability. Presently, MIONPs synthesis by the green approach has received major attention for their non-toxic and eco-friendly properties. However, further research is essential towards a better understanding of their mode of action. In addition, their in-vivo bioactivity studies are needed to be conducted along with extensive toxicity assessments. There is a great need for optimizing the processing factors that may affect their synthesis process along with their prospective applications in healthcare. The development of large-scale production methods of green synthesized IONPs, currently being a big challenge in this field, should be the future research focus.

References

1. Ramos AP, Cruz MA, Tovani CB, Ciancaglini P. Biomedical applications of nanotechnology. Biophys Rev 2017;9:79–89.

2. Saif S, Tahir A, Chen Y. Green synthesis of iron nanoparticles and their environmental applications and implications. Nanomaterials (Basel) 2016;6:209.

3. Akbarzadeh A, Samiei M, Davaran S. Magnetic nanoparticles: preparation, physical properties, and applications in biomedicine. Nanoscale Res Lett 2012;7:144.

4. Yew Y, Shameli K, Miyake M, Khairudin N, Mohamad S, Lee K, *et al.* Green biosynthesis of Superparamagnetic magnetite nanoparticles and biomedical applications in targeted anticancer drug delivery system: A review. Arab J Chem 2020;13:2287–308.

5. Orel VE, Tselepi M, Mitrelias T, Zabolotny M, Shevchenko A, Rykhalskyi A, *et al.* The comparison between superparamagnetic and ferromagnetic iron oxide nanoparticles for cancer nanotherapy in the magnetic resonance system. Nanotechnology 2019;30:415701.

6. Guo T, Lin M, Huang J, Zhou H, Tian W, Yu H, *et al.* The recent advances of magnetic nanoparticles in medicine. J Nanomater 2018;8:1–8.

7. Hasany S, Abdurahman NH, Sunarti AR, Jose R. Magnetic Iron oxide nanoparticles: chemical synthesis and applications review. Curr Nanosci 2013;9:561–75.

8. Rane A, Kanny K, Abitha V, Thomas S. Methods for the synthesis of nanoparticles and fabrication of nanocomposites. In: Bhagyaraj SM, Oluwafemi OS, Kalarikkal N, Thomas S, editors. Micro and Nano Technologies, Synthesis of Inorganic Nanomaterials. Sawston, UK: Woodhead Publishing; 2018. p.121-39.

9. Modan E, Plaiasu A. Advantages and disadvantages of chemical methods in the elaboration of nanomaterials. Metallurgy and Materials Science; 2020 [Internet]. Available from: https://www.gup.ugal.ro/ugaljournals/index.php/mms/article/view/3322 [cited 2021, Nov 23].

10. Ge S, Shi X, Sun K, Li C, Baker JR, Banaszak Holl MM, *et al.* A Facile Hydrothermal Synthesis of Iron Oxide Nanoparticles with Tunable Magnetic Properties. J Phys Chem C 2009;113:13593–9.

11. Majidi S, Sehrig FZ, Farkhani SM, Goloujeh MS, Akbarzadeh A. Current methods for synthesis of magnetic nanoparticles. Artif Cells Nanomed Biotechnol 2016;44:722–34.

12. Wang Y, Nkurikiyimfura I, Pan Z. Sonochemical synthesis of magnetic nanoparticles. Chem Eng Commun 2015;616–21.

13. Lassenberger A, Grünewald TA, van Oostrum PD, Rennhofer H, Amenitsch H, Zirbs R, *et al.* Monodisperse Iron Oxide Nanoparticles by Thermal Decomposition: Elucidating Particle Formation by Second-Resolved in Situ Small-Angle X-ray Scattering. Chem Mater 2017;29:4511–22.

14. Gul S, Khan S, Rehman I, Khan M. A comprehensive review of magnetic nanomaterials modern-day theranostics. Front Mater 2019;19:00179.

15. Strobel R, Pratsinis SE. Direct synthesis of Maghemite, magnetite and wustite nanoparticles by flame spray pyrolysis. Adv Powder Technol 2009;20:190–4.

16. Singh J, Dutta T, Kim KH, Rawat M, Samddar P, Kumar P. 'Green' synthesis of metals and their oxide nanoparticles: applications for environmental remediation. J Nanobiotechnology 2018;16:84.

17. Vitta Y, Figueroa M, Calderon M, Ciangherotti C. Synthesis of iron nanoparticles from aqueous extract of Eucalyptus robusta and evaluation of antioxidant and antimicrobial activity. Mater Sci Energy Technol 2019;3:97–103.

18. Sathishkumar G, Logeshwaran V, Sarathbabu S, Jha PK, Jeyaraj M, Rajkuberan C, *et al.* Green synthesis of magnetic Fe3O4 nanoparticles using Couroupita guianensis Aubl. fruit extract for their antibacterial and cytotoxicity activities. Artif Cells Nanomed Biotechnol 2018;46:589–98.

19. Asoufi H, Antary T, Awwad A. Magnetic nanoparticles synthesis and antigreen peach aphid activity. Journal of chemistry and biochemistry 2018;6:9-16.

20. Aisida S, Madubuonu N, Ezema F. Biogenic synthesis of iron oxide nanorods using Moringa oleifera leaf extract for antibacterial applications. Appl Nanosci 2019;10:305–15.

21. Zambari N, Taib N, Latif F, Mohamed Z. Green synthesis of iron oxide nanoparticles using Azadirachta indica aqueous leaf extract; 2019 [Internet]. Available from: https://www.sciencepubco.com/index.php/ijet/article/view/21811 [cited 2021, Nov 23].

22. Sivakami M, Devi K, Renuka R, Thilagavathi T. Green synthesis of magnetic nanoparticles via Cinnamomum verum bark extract for biological application. J Environ Chem Eng 2020;8:104420.

23. Saranya S, Vijayarani K, Pavithra S. Green synthesis of iron nanoparticles using aqueous extract of Musa ornata flower sheath against pathogenic bacteria. Indian J Pharm Sci 2017;79:688–94.

24. Jegadeesan B, Srimathi K, Srinivas N, Manishkanna S, Vignesh D.

Green synthesis of iron oxide nanoparticles using Terminalia bellirica and Moringa oleifera fruit and leaf extract: Antioxidant, antibacterial, and Thermoacoustic properties. Biocatalysts and agricultural biotechnology 2019;21:101354.

25. Malarkodi C, Malik V, Uma S. Synthesis of Fe2O3 using Emblica officinalis extract and its photocatalytic efficiency. Mater Sci 2018;16:125.

26. Razack S, Suresh A, Sriram S, Ramakrishnan G. Green synthesis of iron oxide nanoparticles using Hibiscus rosa-sinensis for fortifying wheat biscuits. SN Applied Sciences 2020;2:898.

27. Rath K, Sen S. Garlic extract-based preparation of size-controlled Superparamagnetic hematite nanoparticles and their cytotoxic applications. Indian J Biotechnol 2019;18:108–18.

28. Phumying S, Labuayai S, Thomas C, Amornkitbamrung V, Swatsitang E, Maensiri S. Aloe vera plant extracted solution hydrothermal synthesis and magnetic properties of magnetite nanoparticles. Appl Phys (Berl) 2013;111:1187–93.

29. Abdullah J, Eddine L, Abderrhmane B, Gonzalez M, Guerrero A, Romero A. Green synthesis and characterization of iron oxide nanoparticles by Phoenix Dactylifera leaf extract and evaluation of their antioxidant activity. Sustain Chem Pharm 2020;17:100280.

30. Bhuiyan MS, Miah MY, Paul SC, Aka TD, Saha O, Rahaman MM, *et al.* Green synthesis of iron oxide nanoparticle using Carica papaya leaf extract: application for photocatalytic degradation of remazol yellow RR dye and antibacterial activity. Heliyon 2020;6:e04603.

31. Huang L, Weng X, Chen Z, Megharaj M, Naidu R. Synthesis of iron-based nanoparticles using oolong tea extract for the degradation of malachite green. Spectrochim Acta A Mol Biomol Spectrosc 2014;117:801–4.

32. Daniel K, Vinothini G, Subramanian N, Nehru K, Sivakumar M. Biosynthesis of Cu, ZVI, and Ag nanoparticles using Dodonaea viscosa extract for antibacterial activity of human pathogens. J Nanopart Res 2013;15:1–10.

33. Hamsaveni R, Gupta K, Narayana A, Lokesh S. Green synthesis of α-Fe2O3 nanoparticles using Murraya koenigii extract. Solid State Technol 2020;63.

34. Jeyasundari J, Praba P, Brightson Y, Jacob B. Green synthesis and characterization of zero-valent iron nanoparticles from the leaf extract of Psidium guajava plant and their antibacterial activity. Chemical science review and letters 2017;6:1244-52.

35. Senthil M, Ramesh C. Biogenic synthesis of Fe3O4 nanoparticles using tridax procumbens leaf extract and its antibacterial activity on Pseudomonas aeruginosa. Dig J Nanomater Biostruct 2012;7:1655–61.

36. Narayanan S, Sathy BN, Mony U, Koyakutty M, Nair SV, Menon D. Biocompatible magnetite/gold nanohybrid contrast agents via green chemistry for MRI and CT bioimaging. ACS Appl Mater Interfaces 2012;4:251–60.

37. Suganya D, Rajan M, Ramesh R. Green synthesis of iron oxide nanoparticles from leaf extract of Passiflora foetida and its antibacterial activity. Int J Curr Res 2016;42081–5.

38. Madbouly A, Hamdan T. Biosynthesis of magnetite nanoparticles by bacteria. Am j nano research and application 2014;2:98-103.

39. Gonzalez T, Lopez C, Neal A, Perez F, Navarro A, Vivas F, *et al.* Magnetite biomineralization induced by Shewanella oneidensis. Geochim Cosmochim Acta 2010;74:967–79.

40. Torabian P, Ghandehari F, Fatemi M. Biosynthesis of iron oxide nanoparticles by cytoplasmic extracts of bacteria lactobacillus casei. Asian journal of green chemistry 2018;181-8.

41. Zhou W, He W, Zhong S, Wang Y, Zhao H, Li Z, *et al.* Biosynthesis and magnetic properties of mesoporous Fe3O4 composites. J Magn Magn Mater 2009;321:1025–8.

42. Becerra R, Zorrilla C, Ascencio J. Production of iron oxide nanoparticles by a biosynthesis method: an environmentally friendly route. J Phys Chem C 2007;111:16147–53.

43. Abdeen M, Sabry S, Ghozlan H, Gendy A, Carpenter E. Microbial-physical synthesis of Fe and Fe3O4 magnetic nanoparticles using Aspergillus niger YESM1 and supercritical condition of ethanol. J Nanomater 2016;2016:1–8.

44. Demir A, Topkaya R, Baykal A. Green synthesis of Superparamagnetic Fe3O4 nanoparticles with maltose: its magnetic investigation. Polyhedron 2013;65:282–7.

45. Nene A, Takahashi M, Wakita K, Umeno M. Size controlled synthesis of Fe3O4 nanoparticles by ascorbic acid mediated reduction of Fe (acac) 3 without using capping agent. J Nano Res 2016;40:1661–9897.

46. Daldrup-Link HE. Ten Things You Might Not Know about Iron Oxide Nanoparticles. Radiology 2017;284:616–29.

47. Jameel M, Aziz A, Dheyab M. Green synthesis: Proposed mechanism and factors influencing the synthesis of platinum nanoparticles. Green processing and synthesis 2020;41:386-98.

48. Bibi I, Nazar N, Ata S, Sultan M, Ali A, Abbas A, *et al.* Green synthesis of iron oxide nanoparticles using pomegranate seeds extract and photocatalytic activity evaluation for the degradation of textile dye. J Mater Res Technol 2019;8:6115–24.

49. Baumgartner J, Dey A, Bomans PH, Le Coadou C, Fratzl P, Sommerdijk NA, *et al.* Nucleation and growth of magnetite from solution. Nat Mater 2013;12:310–4.

50. Ebrahiminezhad A, Zare-Hoseinabadi A, Sarmah AK, Taghizadeh S, Ghasemi Y, Berenjian A. Plant-Mediated Synthesis and Applications of Iron Nanoparticles. Mol Biotechnol 2018;60:154–68.

51. Park Y, Hong YN, Weyers A, Kim YS, Linhardt RJ. Polysaccharides and phytochemicals: a natural reservoir for the green synthesis of gold and silver nanoparticles. IET Nanobiotechnol 2011;5:69–78.

52. Lynch I, Cedervall T, Lundqvist M, Cabaleiro-Lago C, Linse S, Dawson KA. The nanoparticle-protein complex as a biological entity; a complex fluids and surface science challenge for the 21st century. Adv Colloid Interface Sci 2007;134-135:167–74.

53. Mou X, Ali Z, Li S, He N. Applications of magnetic nanoparticles in targeted drug delivery system. J Nanosci Nanotechnol 2015;15:54–62.

54. Ayubi M, Karimi M, Abdpour S, Rostamizadeh K, Parsa M, Zamani M, *et al.* Magnetic nanoparticles decorated with PEGylated curcumin as dual targeted drug delivery: Synthesis, toxicity and biocompatibility study. Mater Sci Eng C 2019;104:109810.

55. Sirivat A, Paradee N. Facile synthesis of gelatin-coated Fe3O4 nanoparticle: effect of pH in single-step co-precipitation for cancer drug loading. Mater Des 2019;181:264–1275.

56. Prabha G, Raj V. Formation and characterization of β-cyclodextrin (β-CD) - polyethyleneglycol (PEG) - polyethyleneimine (PEI) coated Fe3O4 nanoparticles for loading and releasing 5-Fluorouracil drug. Biomed Pharmacother 2016;80:173–82.

57. Aliabadi M, Shagholani H, Yunessnia Lehi A. Synthesis of a novel biocompatible nanocomposite of graphene oxide and magnetic nanoparticles for drug delivery. Int J Biol Macromol 2017;98:287–91.

58. Wang D, Zhou J, Chen R, Shi R, Xia G, Zhou S, *et al.* Magnetically guided delivery of DHA and Fe ions for enhanced cancer therapy based on pH-responsive degradation of DHA-loaded Fe3O4@C@MIL-100(Fe) nanoparticles. Biomaterials 2016;107:88–101.

59. Mashhadi Malekzadeh A, Ramazani A, Tabatabaei Rezaei SJ, Niknejad H. Design and construction of multifunctional hyperbranched polymers coated magnetite nanoparticles for both targeting magnetic resonance imaging and cancer therapy. J Colloid Interface Sci 2017;490:64–73.

60. Barahuie F, Dorniani D, Saifullah B, Gothai S, Hussein MZ, Pandurangan AK, *et al.* Sustained release of anticancer agent phytic acid from its chitosan-coated magnetic nanoparticles for drug-delivery system. Int J Nanomedicine 2017;12:2361–72.

61. Pham X, Nguyen T, Pham T, Tran T, Tran T. Synthesis and characterization of chitosan-coated magnetite nanoparticles and their application in curcumin drug delivery. Advances in natural sciences: Nanoscience and nanotechnology 2016;7:2043-6262.

62. Rehana D, Haleel A, Rahiman A. Hydroxy, carboxylic and ami-

noacid functionalized Superparamagnetic iron oxide nanoparticles: Synthesis, characterization and in vitro anticancer studies. J Chem Sci 2015;•••:1155–66.

63. Javid A, Ahmadian S, Saboury AA, Kalantar SM, Rezaei-Zarchi S, Shahzad S. Biocompatible APTES-PEG modified magnetite nanoparticles: effective carriers of antineoplastic agents to ovarian cancer. Appl Biochem Biotechnol 2014;173:36–54.

64. Abenojar E, Wickramasinghe S, Concepcion J, Samia A. Structural effects on the magnetic hyperthermia properties of iron oxide nanoparticles. Prog Nat Sci 2016;26:440–8.

65. Wani KD, Kadu BS, Mansara P, Gupta P, Deore AV, Chikate RC, *et al.* Synthesis, characterization and in vitro study of biocompatible cinnamaldehyde functionalized magnetite nanoparticles (CPGF Nps) for hyperthermia and drug delivery applications in breast cancer. PLoS One 2014;9:e107315.

66. Tomitaka. A, Yamada T, Takemura Y. Magnetic nanoparticle hyperthermia using pluronic coated Fe3O4 nanoparticles: an invitro study. Journal of nanomaterials 2012; 2012.

67. Nunez A, Garcia L, Goya G, Sanz B, Salazar S. In-vitro magnetic hyperthermia using polyphenol coated Fe3O4 nanoparticles from Cinnamomum verum and Vanilla planifolia: the concert of green synthesis and therapeutic possibilities. Nanotechnology 2018:29.

68. Guardia P, Di Corato R, Lartigue L, Wilhelm C, Espinosa A, Garcia-Hernandez M, *et al.* Water-soluble iron oxide nanocubes with high values of specific absorption rate for cancer cell hyperthermia treatment. ACS Nano 2012;6:3080–91.

69. Hayashi K, Ono K, Suzuki H, Sawada M, Moriya M, Sakamoto W, *et al.* One-Pot Bio functionalization of Magnetic Nanoparticles via Thiol-Ene Click Reaction for Magnetic Hyperthermia and Magnetic Resonance Imaging. Chem Mater 2010;22:3768–72.

70. Prasad N, Rathinasamy K, Panda D, Bahadur D. Mechanism of cell death induced by magnetic hyperthermia with nanoparticles of c-MnxFe2-xO3 synthesized by a single step process. J Mater Chem 2007;5042–51.

71. Le Renard P, Lortz R, Senatore C, Rapin J, Buchegger F, Petri-Fink A, *et al.* Magnetic and in vitro heating properties of implants formed in situ from injectable formulations and containing superparamagnetic iron oxide nanoparticles (SPIONs) embedded in silica microparticles for magnetically induced local hyperthermia. J Magn Magn Mater 2011;323:1054–63.

72. Kim DH, Kim KN, Kim KM, Lee YK. Targeting to carcinoma cells with chitosan- and starch-coated magnetic nanoparticles for magnetic hyperthermia. J Biomed Mater Res A 2009;88:1–11.

73. Asín L, Ibarra MR, Tres A, Goya GF. Controlled cell death by magnetic hyperthermia: effects of exposure time, field amplitude, and nanoparticle concentration. Pharm Res 2012;29:1319–27.

74. Chalkidou A, Simeonidis K, Angelakeris M, Samaras T, Martinez C, Balcells L, *et al.* In vitro application of Fe/MgO nanoparticles as magnetically mediated hyperthermia agents for cancer treatment. J Magn Magn Mater 2011;323:775–80.

75. Xu Y, Wang A, Mao H. Recent developments in magnetic iron oxide nanoparticles for non-invasive bioimaging. Materials matters 2019;14.

76. Shen Z, Wu A, Chen X. Iron Oxide Nanoparticle Based Contrast Agents for Magnetic Resonance Imaging. Mol Pharm 2017;14:1352–64.

77. Dulińska-Litewka J, Łazarczyk A, Hałubiec P, Szafrański O, Karnas K, Karewicz A. Superparamagnetic iron oxide nanoparticles—current and prospective medical applications. Materials (Basel) 2019;12:617.

78. Lee HY, Li Z, Chen K, Hsu AR, Xu C, Xie J, *et al.* PET/MRI dual-modality tumor imaging using arginine-glycine-aspartic (RGD)-conjugated radiolabeled iron oxide nanoparticles. J Nucl Med 2008;49:1371–9.

79. Xie H, Zhu Y, Jiang W, Zhou Q, Yang H, Gu N, *et al.* Lactoferrin-conjugated superparamagnetic iron oxide nanoparticles as a specific MRI contrast agent for detection of brain glioma in vivo. Biomaterials 2011;32:495–502.

80. Su X, Chan C, Shi J, Tsang MK, Pan Y, Cheng C, *et al.* A graphene quantum dot@Fe3O4@SiO2 based nanoprobe for drug delivery sensing and dual-modal fluorescence and MRI imaging in cancer cells. Biosens Bioelectron 2017;92:489–95.

81. Xie J, Chen K, Huang J, Lee S, Wang J, Gao J, *et al.* PET/NIRF/MRI triple functional iron oxide nanoparticles. Biomaterials 2010;31:3016–22.

82. Huang Y, Mao K, Zhang B, Zhao Y. Superparamagnetic iron oxide nanoparticles conjugated with folic acid for dual target-specific drug delivery and MRI in cancer theranostics. Mater Sci Eng C 2017;70:763–71.

83. Ahmadpoor F, Masood A, Feilu N, Parak W, Shojaosadati A. The effect of the surface coating of iron oxide nanoparticles on magnetic resonance imaging relaxivity. Front Nanotechnol 2021;3:644734.

84. Li J, He Y, Sun W, Luo Y, Cai H, Pan Y, *et al.* Hyaluronic acid-modified hydrothermally synthesized iron oxide nanoparticles for targeted tumor MR imaging. Biomaterials 2014;35:3666–77.

85. Mohapatra J, Mitra A, Tyagi H, Bahadur D, Aslam M. Iron oxide nanorods as high-performance magnetic resonance imaging contrast agents. Nanoscale 2015;7:9174–84.

86. Wabler M, Zhu W, Hedayati M, Attaluri A, Zhou H, Mihalic J, *et al.* Magnetic resonance imaging contrast of iron oxide nanoparticles developed for hyperthermia is dominated by iron content. Int J Hyperthermia 2014;30:192–200.

87. Bakhtiary Z, Saei AA, Hajipour MJ, Raoufi M, Vermesh O, Mahmoudi M. Targeted superparamagnetic iron oxide nanoparticles for early detection of cancer: possibilities and challenges. Nanomedicine 2016;12:287–307.

88. De Haro LP, Karaulanov T, Vreeland EC, Anderson B, Hathaway HJ, Huber DL, *et al.* Magnetic relaxometry as applied to sensitive cancer detection and localization. Biomed Tech (Berl) 2015;60:445–55.

89. Kanagesan S, Hashim M, Tamilselvan S, Ismail I, Hajalilou A, Ahsanul K, *et al.* Synthesis, characterization, and cytotoxicity of iron oxide nanoparticles. Advances in materials science and engineering 2013;2013.

90. Das S, Diyali S, Vinothini G, Perumalsamy B, Balakrishnan G, Ramasamy T, *et al.* Synthesis, morphological analysis, antibacterial activity of iron oxide nanoparticles and the cytotoxic effect on lung cancer cell line. Heliyon 2020;6:e04953.

91. Shah ST, A Yehya W, Saad O, Simarani K, Chowdhury Z, A Alhadi A, *et al.* Surface Functionalization of Iron Oxide Nanoparticles with Gallic Acid as Potential Antioxidant and Antimicrobial Agents. Nanomaterials (Basel) 2017;7:306.

92. Neupane BP, Chaudhary D, Paudel S, Timsina S, Chapagain B, Jamarkattel N, *et al.* Himalayan honey loaded iron oxide nanoparticles: synthesis, characterization and study of antioxidant and antimicrobial activities. Int J Nanomedicine 2019;14:3533–41.

93. Sandhya J, Kalaieselvam S. Biogenic synthesis of magnetic iron oxide nanoparticles using inedible Borassus flabellifer seed coat: characterization, antimicrobial, antioxidant activity, and in vitro cytotoxicity analysis. Mater Res Express 2020;7:1591–2053.

94. Lakshminarayanan S, Shereen MF, Niraimathi KL, Brindha P, Arumugam A. One-pot green synthesis of iron oxide nanoparticles from Bauhinia tomentosa: characterization and application towards synthesis of 1, 3 diolein. Sci Rep 2021;11:8643.

95. Yusefi M, Shameli K, Ali R, Pang S, Teow S. Evaluating anticancer activity of plant mediated synthesized iron oxide nanoparticles using Punica granatum fruit peel extract. J Mol Struct 2020;1204:127539.

96. Naseem T, Farrukh M. Antibacterial activity of green synthesis of iron nanoparticles using Lawsonia inermis and Gardenia jasminoides leaves extract. Journal of chemistry 2015;2015.

97. Vasantharaj S, Sathiyavimal S, Senthilkumar P, LewisOscar F, Pugazhendhi A. Biosynthesis of iron oxide nanoparticles using leaf extract of Ruellia tuberosa: antimicrobial properties and their applications in photocatalytic degradation. J Photochem Photobiol B 2019;192:74–82.

98. Arokiyaraj S, Saravanan M, Prakash N, Arasu M, Vijayakumar

B, Vincent S. Enhanced antibacterial activity of iron oxide magnetic nanoparticles treated with Argemone Mexicana leaf extract: an in vitro study. Mater Res Bull 2013;48:3323–7.

99. Pallela PN, Ummey S, Ruddaraju LK, Gadi S, Cherukuri CS, Barla S, *et al.* Antibacterial efficacy of green synthesized α-Fe2O3 nanoparticles using Sida cordifolia plant extract. Heliyon 2019;5:e02765.

Conflicts of interest.—The authors certify that there is no conflict of interest with any financial organization regarding the material discussed in the manuscript.

Authors' contributions.—All authors read and approved the final version of the manuscript.

History.—Manuscript accepted: November 17, 2021. - Manuscript revised: October 21, 2021. – Manuscript received: June 16, 2021.

Supplementary data.—For supplementary materials, please see the HTML version of this article at www.minervamedica.it